Bandwidth-Constrained Decentralized Detection of an Unknown Vector Signal via Multisensor Fusion

Domenico Ciuonzo ⬤, *Senior Member, IEEE*, S. Hamed Javadi ⬤, *Member, IEEE*,
Abdolreza Mohammadi ⬤, *Member, IEEE*, and Pierluigi Salvo Rossi ⬤, *Senior Member, IEEE*

Abstract—Decentralized detection is one of the key tasks that a wireless sensor network (WSN) is faced to accomplish. Among several decision criteria, the Rao test is able to cope with an unknown (but parametrically-specified) sensing model, while keeping computational simplicity. To this end, the Rao test is employed in this paper to fuse multivariate data measured by a set of sensor nodes, each observing the target (or the desired) event via a nonlinear mapping function. In order to meet stringent energy/bandwidth requirements, sensors quantize their vector-valued observations into one or few bits and send them over error-prone (to model low-power communications) reporting channels to a fusion center (FC). Therein, a global (better) decision is taken via the proposed test. Its closed form and asymptotic (large-size WSN) performance are obtained, and the latter leveraged to optimize quantizers. The appeal of the proposed approach is confirmed via simulations.

Index Terms—Data fusion, decentralized detection, generalized likelihood ratio test (GLRT), Internet of Things (IoT), rao test, threshold optimization, WSNs.

I. INTRODUCTION

A. Motivation

DECENTRALIZED detection with wireless sensor networks (WSNs) has become a deeply researched area in the last decades [1]–[3]. Due to energy and bandwidth limitations, each node, rather than sending its observed measurements, compresses them into one-bit of information about the estimated hypothesis to a fusion center (FC), which is in charge of taking a global decision about either the occurrence of a *phenomenon of interest* (hypothesis $\mathcal{H}_1$, representing e.g. an anomaly) or the null

hypothesis $\mathcal{H}_0$. The optimal decision test (under Bayesian and Neyman-Pearson frameworks) at each sensor is well known to be a one-bit quantization of the local likelihood ratio test (LRT) [1]. However, in most practical cases, the LRT at the generic sensor node cannot be evaluated due to an incompletely-specified sensing model. Besides, even when the nodes can compute their local LRT, the search for local quantization thresholds is well known to be an exponentially complex problem [4].

In such scenarios, the raw measurement (vector) is directly (compressed and) quantized into one-bit of information. Hence, to cope with the presence of unknown parameters, the FC is demanded to solve a composite hypothesis testing problem to capitalize the spatial diversity provided by the WSN (encoded into the received bits) [5], [6]. The above task both requires high performance and acceptable complexity, in order to reduce the processing power of the FC. Indeed, the latter may be also battery-powered and represent the cluster head (intermediate node) of a hierarchical fusion architecture [7], [8].

B. Related Works

As previously mentioned, the *sensing model* statistics of the desired signal may be practically not available in nodes. Such challenging situation has a direct implication on (a) the design of the fusion rules at the FC, which in turn depend on (b) the type of local sensor processing.

On one hand, there is a corpus of literature dealing with the design of simple fusion approaches, which practically neglect the dependence with respect to (w.r.t) the unknown signal, such as the well-known counting rule [9], [10] (which enjoys remarkable robustness [11] and invariance [12] properties) or channel-aware (but relying on ideal sensor assumption) decision statistics [13], [14]. On the other hand, in some particular scenarios [15] the uniformly most powerful test is independent of the unknown parameters; thus, they do not need to be estimated.

Nonetheless, when neglecting the dependence on unknown parameters at design phase leads to unacceptable performance degradation, the *generalized likelihood ratio test* (GLRT) is usually capitalized as the building rationale to design the fusion rule. Accordingly, GLRT-based fusion of quantized data was studied in [16], [17] and [18] for detecting a source with unknown location by passive/active methods, and fusing conditionally-dependent decisions, respectively. Additionally, the GLRT has been leveraged in [6] to detect an unknown deterministic signal through a WSN reporting one-bit quantized measurements via

Domenico Ciuonzo is with the Department of Electrical Engineering and Information Technologies (DIETI), University of Naples Federico II, 80125 Naples, Italy (e-mail: domenico.ciuonzo@unina.it).

S. Hamed Javadi is with the Department of Environment, Ghent University, 9000 Ghent 9000, Belgium, and also with the Department of Electrical Engineering, University of Bojnord, Bojnord 9179155954, Iran (e-mail: s.h.javadi@ieee.org).

Abdolreza Mohammadi is with the Department of Electrical Engineering, University of Bojnord, Bojnord 9179155954, Iran (e-mail: a.mohammadi@ub.ac.ir).

Pierluigi Salvo Rossi is with the Department of Electronic Systems, Norwegian University of Science and Technology (NTNU), 7491 Trondheim, Norway (e-mail: salvorossi@ieee.org).

Digital Object Identifier 10.1109/TSIPN.2020.3037832

TABLE I
CATEGORIZATION OF CLOSELY-RELATED WORKS ON DECENTRALIZED DETECTION WITH UNKNOWN PARAMETERS. LEGEND:
VM (VECTOR MEASUREMENT): ○ (SCALAR MEASUREMENT); ● (VECTOR MEASUREMENT);
VP (VECTOR PARAMETER): ○ (SCALAR PARAMETER); ● (VECTOR PARAMETER);
NLM (NON-LINEAR MODEL): ○ (LINEAR MODEL); ◐ (NON-LINEAR MODEL WITH LINEAR DEPENDENCE IN THE
UNKNOWN PARAMETERS); ● (NON-LINEAR MODEL);
Q (QUANTIZATION): ○ (NO QUANTIZATION); ◐ (ONE-BIT QUANTIZATION); ● (MULTI-BIT QUANTIZATION);
RC (REPORTING CHANNELS): ○ (IDEAL); ● (NOISY); **FUSION RULE**: GLR (GENERALIZED LIKELIHOOD RATIO); LoD (LOCALLY-OPTIMUM DETECTION).

Paper	VM	VP	NLM	Q	RC	Fusion Rule
Fang *et al.*, 2013 [6]	○	○	○	◐	○	GLR
Fang *et al.*, 2014 [33]	●	●	○	○	○	GLR
Ciuonzo *et al.*, 2014 [5]	○	○	○	◐	●	Rao
Ciuonzo *et al.*, 2017 [25]	○	○	◐	◐	●	Rao
Hu *et al.*, 2018 [27]	○	○	◐	◐	●	GLR/Rao
Cheng *et al.*, 2019 [24]	○	○	○	●	●	Rao
Wang *et al.*, 2019 [29]	○	○	○	●	○	LoD
Wang *et al.*, 2019 [30]	○	○	○	●	○	LoD
Hu *et al.*, 2020 [17]	○	●	●	●	●	GLR
Cheng *et al.*, 2020 [26]	○	○	◐	●	●	GLR/Rao
This paper	●	●	●	●	●	GLR/Rao

noisy communication channels; this fusion rule has been then extended to cope with multi-bit measurements in [19]. Recent interesting applications of the GLRT also include distributed detection of arbitrarily-permuted one-bit quantized data [20], sparse signals [21] and one-bit quantized data in a sequential setup [22].

Conversely, the *Rao test* [23] does not require maximum likelihood estimates under the alternative hypothesis ($\mathcal{H}_1$). Hence, it represents a simpler detection method for tackling composite hypothesis testing, while asymptotically yielding the same performance as the GLRT. Accordingly, several works appeared leveraging Rao test in WSN-based detection [5], [24]–[28] and, in general, score tests [29], [30] (due to analogous advantages). For example, Ciuonzo *et al.* [5] have proposed a Rao fusion rule based on one-bit quantization of scalar measurements, whereas a corresponding generalization to multi-bit case has been devised in [24]. Recently, its simplicity has been exploited to detect an uncooperative target (e.g. with also unknown location) at the FC, by developing a generalized version of the test (i.e. the supremum of a family of target-location-dependent Rao statistics) for the one-bit [25] and multi-bit cases [26]. The uncooperative-target case has been recently analyzed also in an online setup with a sequential version of the above fusion (one-bit) rule [27]. Furthermore, [28], [31] have applied the Rao test to collision-aware reporting for fusion design. Finally, locally most-powerful tests have been applied to decentralized detection of sparse signals in (generalized) Gaussian noise [29], [30].

It is worth noticing that all the above works have dealt only with (single- or multi-level) quantized versions of a scalar measurement (x_k) at each sensor [5], [6], [24]–[27]. Differently, when each sensor node has available a vector of measurements ($\boldsymbol{x}_k$), it has been suggested in [32], [33] (for estimation and detection tasks, respectively) to compress its observations using a linear precoder. By using a linear precoder, the vector-valued observation of the kth node, $\boldsymbol{x}_k$, is converted to a scalar $\boldsymbol{c}_k^T \boldsymbol{x}_k$ before transmission, where $\boldsymbol{c}_k$ is a compression vector. However, in the work [33], no quantization issues were taken into account and a GLRT fusion rule was designed based on real-valued (infinite-bandwidth) compressed measurements. On the other hand, Fang et Li [32] considered also one-bit quantization of the resulting scalar measurement for estimation purposes. In the latter case, the combined compression-quantization strategy is referred to as *hyperplane-based quantizer*, because of its geometrical interpretation. It is worth noticing that in the above corpus of literature *only linear sensing models have been considered*. The above considerations are condensed within Table I, which categorizes related works on decentralized detection with unknown parameters (viz. composite hypotheses) along the main distinctive features so as to highlight the novelty of our work.

Accordingly, the design of (detection) fusion rules (a) in the vector case, (b) based on a non-linear sensing model and (c) with both compression & quantization (hyperplane-based quantizers) *appears unexplored*, to the best of our knowledge.

C. Summary of Contributions and Manuscript Organization

The contributions of this paper are summarized as follows:
- We study distributed detection by sensor fusion of data from network nodes for (i) a general (e.g. non-linear) vector measurement model, (ii) sensors employing hyperplane-based quantizers, (iii) imperfect communication channels with non-identical per-sensor bit error probabilities and (iv) no knowledge of the desired vector signal determining the hypothesis. As a byproduct of our study, the linear

scalar and vector valued measurement models are investigated as special cases.

- After investigating the GLRT for the above general model, we explicitly derive the Rao test as a computationally simpler alternative, namely having the appeal of being in *closed-form*. The corresponding Rao fusion rule comprises the scalar counterpart in [5] as a *special case* and represents an appealing method for decision fusion from multimodal (vector-valued) sensors with limited bandwidth and energy requirements.

- We provide the asymptotic performance of Rao (viz. GLRT) fusion rule with respect to the number of sensors. Leveraging its explicit expression, we pursue an asymptotically-optimal design for hyperplane-based quantizers (e.g. the design of both the compression vector c_k and the quantizer threshold τ_k) which aims at maximizing the corresponding *non-centrality parameter* [23]. It is shown that, while an explicit optimized expression can be obtained for the optimal $\tau_k^\star$ (in general, depending on the particular c_k chosen), the optimal compression vector $c_k^\star$ depends on the unknown vector signal $\boldsymbol{\theta}$. Hence, we resort to different sub-optimal, but reasonable, heuristics for its design.

- The above results for one-bit hyperplane-based quantizers are then extended to the case of *multi-bit* quantization for each sensor, following the assumptions in [34]. The corresponding multi-bit Rao fusion rule retains the same implementation simplicity, while generalized heuristic choices are carried out for compression matrix design.

- The Rao test is compared to the GLRT through simulations showing that, other than sharing the same asymptotic distribution, it achieves practically the same performance for a finite number of sensors. To make the comparison complete, also (upper-bound) *baselines* are here considered. Finally, performance trends w.r.t. relevant WSN parameters are investigated.

The paper is organized as follows: Section II describes the measurement and communication channel models used, along with the quantization method employed. The GLRT and Rao fusion rules are formulated in Section III, while the parameter design of local sensors is discussed in Section IV. The one-bit quantizers and the related Rao test are extended to the general multi-bit case in Section V. Simulation results for validation of our approach are given in Section VI. Finally, Section VII draws conclusions and suggests further avenues of research.

Notation: Lower-case (resp. upper-case) bold letters denote vectors (resp. matrices), with a_k (resp. $a_{n,m}$) representing the kth element (resp. (n, m)th element) of $\boldsymbol{a}$ (resp. $\boldsymbol{A}$); upper-case calligraphic letters, e.g. $\mathcal{A}$, denote finite sets; $\mathbb{E}\{\cdot\}$, $(\cdot)^T$, $\mathrm{tr}(\cdot)$, $(\cdot)^\dagger$, $\langle \cdot, \cdot \rangle$ and $\| \cdot \|$ denote expectation, transpose, matrix trace, Hermitian, inner product and vector Euclidean norm operators, respectively; $\boldsymbol{0}_N$ (resp. $\boldsymbol{1}_N$) denotes the null (resp. ones) vector of length N; $\boldsymbol{I}_n$ denotes the identity matrix of size n; $P(\cdot)$ and $p(\cdot)$ are used to denote probability mass functions (PMF) and probability density functions (PDF); $\mathcal{N}(\boldsymbol{\mu}, \boldsymbol{\Sigma})$ denotes a normal distribution with mean vector $\boldsymbol{\mu}$ and covariance matrix $\boldsymbol{\Sigma}$; $\mathcal{Q}(\cdot)$ is used to denote the complementary cumulative distribution function (CCDF) of standard normal distribution; $\mathcal{U}(a, b)$ denotes
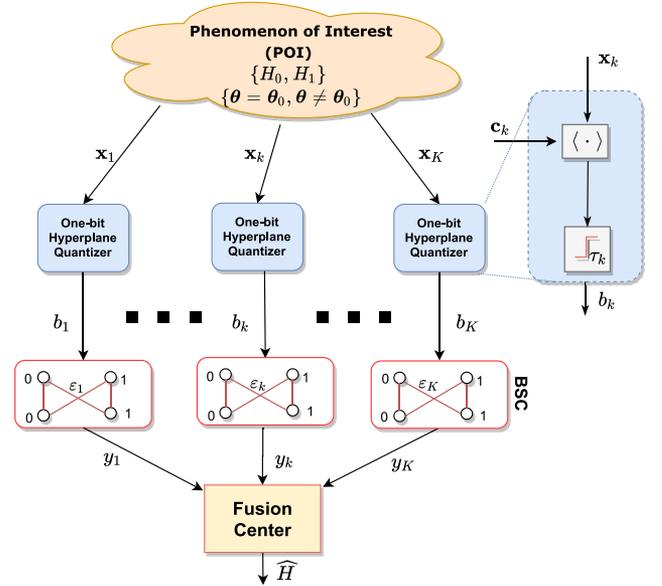

Fig. 1. System model used in this paper. Each sensor compresses its measurement vector via a hyperplane-based quantizer. Each bit is then sent through a binary symmetric channel and received by the FC.

a uniform PDF with support $[a, b]$; χ_k^2 (resp. $\chi_k'^2(\xi)$) denotes a chi-square (resp. a non-central chi-square) distribution with k degrees of freedom (resp. and non-centrality parameter ξ); $u(\cdot) \in \{0, 1\}$ denotes the Heaviside (unit) step function; finally, the symbols $\sim$ and $\overset{a}{\sim}$ mean "distributed as" and "asymptotically distributed as".

II. SYSTEM MODEL

In this work we adopt the system model shown in Fig. 1, which is elaborated throughout this section. Specifically, we first describe the non-linear measurement model (Section II-A) considered. Then, we focus on sensors' compression & quantization method, ending with the communication model employed (Section II-B). Finally, we formulate rigorously the testing problem considered (Section II-C).

A. Measurement Model

We consider a binary hypothesis testing problem in which a collection of sensor nodes $k \in \mathcal{K} \triangleq \{1, \ldots, K\}$ collaborate to reveal an anomalous event, summarized through the unknown deterministic vector parameter $\boldsymbol{\theta} \in \mathbb{R}^p$. In the rest of the paper, we make the assumption $K \geq p$, i.e. there are enough sensors to (implicitly) estimate the unknown vector $\boldsymbol{\theta}$.

More specifically, we assume that the normal behaviour is represented by $\boldsymbol{\theta} = \boldsymbol{\theta}_0$, while any deviation $\boldsymbol{\theta} \neq \boldsymbol{\theta}_0$ denotes an anomaly. The present model encompasses many tasks of interest, such as revealing (in a decentralized fashion) the presence of an unknown target (i.e. $\boldsymbol{\theta}_0 = \boldsymbol{0}_p$).

The measurement model at kth sensor is summarized as follows:

$$\begin{cases} \mathcal{H}_0: & \boldsymbol{x}_k = \boldsymbol{g}_k(\boldsymbol{\theta}_0) + \boldsymbol{w}_k, \\ \mathcal{H}_1: & \boldsymbol{x}_k = \boldsymbol{g}_k(\boldsymbol{\theta}) + \boldsymbol{w}_k, \quad k \in \mathcal{K}; \end{cases} \quad (1)$$

where $\boldsymbol{x}_k \in \mathbb{R}^m$ denotes the kth node measurement vector, $\boldsymbol{g}_k(\cdot): \mathbb{R}^p \to \mathbb{R}^m$ is a known functional (possibly *non-linear*) mapping describing the input-output relationship between the (unknown) parameter vector and the measurement vector for the kth node. Furthermore, $\boldsymbol{w}_k \in \mathbb{R}^m$ denotes the noise vector experienced by kth sensor, modelled as a multivariate zero-mean Gaussian, that is $\boldsymbol{w}_k \sim \mathcal{N}(\mathbf{0}_m, \boldsymbol{\Sigma}_k)$; the random variables (RVs) $\boldsymbol{w}_k$s are here assumed *mutually independent*. Finally, aiming at keeping a compact notation, we collect all the measurements in the vector $\boldsymbol{x} \triangleq [\boldsymbol{x}_1^T \ldots \boldsymbol{x}_K^T]^T \in \mathbb{R}^{mK \times 1}$.

Remarkably, the model in Eq. (1) *comprises many special cases of interest*, as detailed hereinafter.

1) The scalar linear (SL) measurement model: If we just consider a linear model and a scalar-valued parameter to be detected ($\theta_0 = 0$), we obtain

$$\begin{cases} \mathcal{H}_0: & x_k = w_k, \\ \mathcal{H}_1: & x_k = h_k\theta + w_k, \qquad k \in \mathcal{K} \end{cases} \quad (2)$$

where θ is the unknown scalar parameter, h_k is the observation coefficient and $w_k \sim \mathcal{N}(0, \sigma_k^2)$. Such a model was extensively analyzed in decentralized estimation studies [34]–[37] and, recently, in (decentralized) composite hypothesis testing [5], [6], [19], [24].

2) The vector linear (VL) measurement model: Such model is the vector counterpart of Eq. (2) (i.e. $\boldsymbol{\theta}_0 = \mathbf{0}_p$) and can be summarized as follows:

$$\begin{cases} \mathcal{H}_0: & \boldsymbol{x}_k = \boldsymbol{w}_k, \\ \mathcal{H}_1: & \boldsymbol{x}_k = \boldsymbol{H}_k\boldsymbol{\theta} + \boldsymbol{w}_k, \qquad k \in \mathcal{K} \end{cases} \quad (3)$$

where $\boldsymbol{\theta}$ is the unknown vector parameter, $\boldsymbol{H}_k \in \mathbb{R}^{m \times p}$ is a known observation matrix and $\boldsymbol{w}_k$ denotes the noise vector. This problem was considered in decentralized estimation in [32], [34] while a (composite) hypothesis testing was actually considered only in [33] for the special case $\boldsymbol{H}_k = \boldsymbol{I}_p$, adopting (a) a GLRT design as the relevant fusion rule and (b) assuming perfect measurement reporting at the FC (i.e. no quantization).

B. Compression, Quantization and Reporting

In this paper, we will consider a hyperplane-based quantizer, as proposed in [32], [34]. More specifically, to meet stringent bandwidth and power budgets in WSNs, the kth sensor quantizes its observation vector $\boldsymbol{x}_k$ into one bit (b_k) as [32]:

$$b_k \triangleq u\left(\boldsymbol{c}_k^T \boldsymbol{x}_k - \tau_k\right), \quad (4)$$

where $\boldsymbol{c}_k \in \mathbb{R}^m$ is a compression vector used by the kth node to obtain a real-valued scalar and τ_k denotes the kth sensor quantizer threshold (both known at the FC), determining the binary value of the corresponding bit b_k. Hyperplane-based quantizers restrict the partition region to be a half-space whose border is a hyperplane defined by a compression vector $\boldsymbol{c}_k$ and a quantization threshold τ_k. Their appeal lies in their ease of implementation, which is highly-desirable on low-cost sensor devices.

Remark: for the SL model, the expression in Eq. (4) specializes into $b_k \triangleq u(c_k x_k - \tau_k)$. Accordingly, the presence of the scaling term c_k is redundant in the quantization of the SL model and kept *only for notational consistency* in what follows.

Similarly as in [5], [6], [25], we assume that the one-bit quantized measurement b_k is sent over a binary symmetric channel (BSC) and the FC observes an error-prone y_k, that is

$$y_k = \begin{cases} b_k & \text{with probability } 1 - \epsilon_k \\ (1 - b_k) & \text{with probability } \epsilon_k \end{cases} \quad (5)$$

where ϵ_k denotes the (known) bit error probability (BEP) experienced by the node k's link to the FC. Finally, we collect the received data from nodes at the FC as $\boldsymbol{y} \triangleq [y_1 \cdots y_K]^T$.

C. Problem Statement

We highlight that the hypothesis testing described in Eq. (1) represents a *two-sided test* [23], where $\{\mathcal{H}_0, \mathcal{H}_1\}$ corresponds to $\{\boldsymbol{\theta} = \boldsymbol{\theta}_0, \boldsymbol{\theta} \neq \boldsymbol{\theta}_0\}$ and, additionally, the vector parameter $\boldsymbol{\theta}$ is *unknown*. The above task is further complicated by (i) the presence of a possibly non-linear mapping $\boldsymbol{g}_k(\cdot)$ in the sensing process, (ii) the loss of information (an additional non-linearity) due to compression & quantization (based on $\boldsymbol{c}_k$'s and τ_k's) and (iii) the non-ideality of the reporting channels.

Accordingly, the problem considered here is (a) the derivation of a (computationally) simple test (resorting to a decision statistic Λ, which is compared to a decision threshold γ) on the basis of $\boldsymbol{y}$ and (b) the corresponding quantizer design (consisting in a globally-optimal choice of $\boldsymbol{c}_k$'s and τ_k's for each sensor). We remark that the quantizer design in (b) is peculiar to our problem, as the objective typically used in vector quantization corresponds to minimizing the reconstruction error between $\boldsymbol{x}_k$ and its quantized counterpart. Differently, in this paper, the ultimate goal of the WSN is to decide reliably for the actual hypothesis (either $\mathcal{H}_0$ or $\mathcal{H}_1$) in force without necessarily being able to recover the set of sensors measurements.

Finally, the performance will be evaluated in terms of the well-known system (global) probabilities of detection $P_{D_0} \triangleq \Pr\{\Lambda > \gamma | \mathcal{H}_1\}$ and false-alarm $P_{F_0} \triangleq \Pr\{\Lambda > \gamma | \mathcal{H}_0\}$.

III. FUSION RULES DESIGN

This section deals with fusion rules design. Specifically, after obtaining the explicit likelihood function for the hypothesis testing problem at hand (Section III-A), the implicit GLRT expression (Section III-B) and the explicit Rao test form (Section III-C) are obtained, highlighting their specialization to SL/VL models.

A. Likelihood Function

Before proceeding with the design of the considered fusion rules, we compute the explicit (log-) likelihood of the received vector $\boldsymbol{y}$ as a function of $\boldsymbol{\theta}$. We remark that simply setting $\boldsymbol{\theta} = \boldsymbol{\theta}_0$ provides the (log-) probability mass function (PMF) under $\mathcal{H}_0$.

More specifically, by exploiting the independence among nodes' data conditioned on each hypothesis, it can be readily shown that the PMF factorizes as $P(\boldsymbol{y}; \boldsymbol{\theta}) = \prod_{k=1}^{K} P(y_k; \boldsymbol{\theta})$. Then, the contribution of the kth node, through the term $P(y_k; \boldsymbol{\theta})$, is given in closed form as:

$$P(y_k; \boldsymbol{\theta}) = [\psi_k(\boldsymbol{\theta})]^{y_k} [1 - \psi_k(\boldsymbol{\theta})]^{1-y_k}, \quad (6)$$

where $\psi_k(\boldsymbol{\theta}) \triangleq P(y_k = 1; \boldsymbol{\theta})$ denotes the received bit probability. The latter term is explicitly given by:

$$\psi_k(\boldsymbol{\theta}) = \mathcal{Q}\left(\frac{\tau_k - \boldsymbol{c}_k^T \boldsymbol{g}_k(\boldsymbol{\theta})}{\sqrt{\boldsymbol{c}_k^T \boldsymbol{\Sigma}_k \boldsymbol{c}_k}}\right)(1 - 2\epsilon_k) + \epsilon_k \quad (7)$$

Indeed, the useful (scalar) signal $\boldsymbol{c}_k^T \boldsymbol{g}_k(\boldsymbol{\theta})$ is affected by an equivalent noise $v_k \triangleq (\boldsymbol{c}_k^T \boldsymbol{w}_k)$ arising from a linear operation of $\boldsymbol{w}_k$. As a result, it holds $v_k \sim \mathcal{N}(0, \boldsymbol{c}_k^T \boldsymbol{\Sigma}_k \boldsymbol{c}_k)$.

Because of bits' mutual independence, the log-PMF is easily obtained as:

$$\ln P(\boldsymbol{y}; \boldsymbol{\theta}) = \sum_{k=1}^{K} y_k \ln \psi_k(\boldsymbol{\theta}) + (1 - y_k)\ln[1 - \psi_k(\boldsymbol{\theta})] \quad (8)$$

In the following, we investigate the fusion rules based on GLRT and Rao test.

B. GLRT

A common approach to handle detection in the presence of unknown parameters (viz. composite hypothesis testing) resorts to the GLRT [23]. If the GLRT is adopted as the fusion rule at the FC, the implicit expression will be given by:

$$\Lambda_G \triangleq 2\ln\frac{\max_{\boldsymbol{\theta}} P(\boldsymbol{y}; \boldsymbol{\theta})}{P(\boldsymbol{y}; \boldsymbol{\theta}_0)}. \quad (9)$$

The evaluation of the above statistic relies on the log-PMF form provided in Eq. (8) and is complicated by the optimization at the numerator. It is proved that the log-likelihood function is concave in $\boldsymbol{\theta}$ for some relevant cases [32], [35], hence there is only a (unique) global maximum. Still, although computationally-efficient search algorithms can be used to find the global maximum, *a closed form for Eq. (9) cannot be obtained.*

C. Rao Test

An attractive alternative which avoids cumbersome optimization is given by the well-known Rao test [23], as it does not require maximization in the numerator of Eq. (9). The implicit expression for Rao test is given by [23]:

$$\Lambda_R \triangleq \left.\boldsymbol{\delta}^T(\boldsymbol{y}; \boldsymbol{\theta})\right|_{\boldsymbol{\theta}=\boldsymbol{\theta}_0} \boldsymbol{I}^{-1}(\boldsymbol{\theta}_0)\left.\boldsymbol{\delta}(\boldsymbol{y}; \boldsymbol{\theta})\right|_{\boldsymbol{\theta}=\boldsymbol{\theta}_0} \quad (10)$$

where $\boldsymbol{\delta}(\boldsymbol{y}; \boldsymbol{\theta}) \triangleq \frac{\partial \ln P(\boldsymbol{y}; \boldsymbol{\theta})}{\partial \boldsymbol{\theta}}$ is the *score function* and $\boldsymbol{I}(\boldsymbol{\theta}) \triangleq \mathbb{E}\{\boldsymbol{\delta}(\boldsymbol{y}; \boldsymbol{\theta})\boldsymbol{\delta}(\boldsymbol{y}; \boldsymbol{\theta})^T\}$ denotes the *Fisher information matrix* (FIM) as a function of the unknown parameter $\boldsymbol{\theta}$.

In what follows, we obtain the closed-form Rao statistic for the general measurement model in Eq. (1). To this end, we need to evaluate the closed-form expressions of the score vector $\boldsymbol{\delta}(\boldsymbol{y}; \boldsymbol{\theta})$ and the FIM $\boldsymbol{I}(\boldsymbol{\theta})$. The following two propositions will help accomplishing the above task.

Proposition 1: The explicit form of the score vector is:

$$\boldsymbol{\delta}(\boldsymbol{y}; \boldsymbol{\theta}) = \sum_{k=1}^{K} q_k(\boldsymbol{\theta})[y_k - \psi_k(\boldsymbol{\theta})]\boldsymbol{J}_k^T(\boldsymbol{\theta})\boldsymbol{c}_k \quad (11)$$

where

$$\boldsymbol{J}_k(\boldsymbol{\theta}) \triangleq \frac{\partial \boldsymbol{g}_k(\boldsymbol{\theta})}{\partial \boldsymbol{\theta}^T} \quad (12)$$

Algorithm 1: Rao test: Fusion rule evaluation at the FC.

Init Parameters: compression vectors $\boldsymbol{c}_1, \ldots, \boldsymbol{c}_K$; quantization thresholds $\tau_1, \ldots, \tau_K$;

Input: received bits $y_1, \ldots, y_K$.

Output: the estimated hypothesis $\hat{\mathcal{H}}$.

1: **for** $k = 1, \ldots, K$ **do**
2:      Compute $\psi_k(\boldsymbol{\theta})$ and $q_k(\boldsymbol{\theta})$ as Eqs. (7) and (13), respectively;
3: **end for**
4: Compute the score vector $\boldsymbol{\delta}(\boldsymbol{y}; \boldsymbol{\theta})$ as Eq. (11);
5: Compute the FIM $\boldsymbol{I}(\boldsymbol{\theta})$ as Eq. (14);
6: Evaluate Rao statistic Λ_R as Eq. (15);
7: Declare the estimated hypothesis as $\Lambda_R \underset{\hat{\mathcal{H}}=\mathcal{H}_0}{\overset{\hat{\mathcal{H}}=\mathcal{H}_1}{\gtrless}} \gamma$;

---

denotes the Jacobian matrix of $\boldsymbol{g}_k(\boldsymbol{\theta})$, whereas $q_k(\boldsymbol{\theta})$ is defined as

$$q_k(\boldsymbol{\theta}) \triangleq \frac{\zeta_k\, p_{v_k}\left(\tau_k - \boldsymbol{c}_k^T \boldsymbol{g}_k(\boldsymbol{\theta})\right)}{\psi_k(\boldsymbol{\theta})\,(1 - \psi_k(\boldsymbol{\theta}))}. \quad (13)$$

In the above equation, $\zeta_k \triangleq (1 - 2\epsilon_k)$ and $p_{v_k}(\cdot)$ denotes the PDF of v_k.

Proof: See Appendix A.

Proposition 2: The closed form of the FIM is:

$$\boldsymbol{I}(\boldsymbol{\theta}) = \sum_{k=1}^{K}\left\{q_k(\boldsymbol{\theta})^2\,\psi_k(\boldsymbol{\theta})[1 - \psi_k(\boldsymbol{\theta})]\boldsymbol{J}_k^T(\boldsymbol{\theta})\boldsymbol{c}_k\boldsymbol{c}_k^T\boldsymbol{J}_k(\boldsymbol{\theta})\right\}, \quad (14)$$

where $\boldsymbol{J}_k(\boldsymbol{\theta})$ and $q_k(\boldsymbol{\theta})$ retain the same definitions as in Eqs. (12) and (13), respectively.

Proof: See Appendix B. ∎

Therefore, combination of the results in Eqs. (11) and (14) provides the explicit form of the Rao statistic in Eq. (15), reported in what follows

$$\Lambda_R = \left\{\sum_{k=1}^{K}\boldsymbol{c}_k^T\boldsymbol{J}_k(\boldsymbol{\theta}_0)\,q_k(\boldsymbol{\theta}_0)[y_k - \psi_k(\boldsymbol{\theta}_0)]\right\}$$
$$\times \boldsymbol{I}(\boldsymbol{\theta}_0)^{-1}\left\{\sum_{k=1}^{K}q_k(\boldsymbol{\theta}_0)[y_k - \psi_k(\boldsymbol{\theta}_0)]\boldsymbol{J}_k(\boldsymbol{\theta}_0)^T\boldsymbol{c}_k\right\} \quad (15)$$

The algorithmic procedure required for Rao test implementation is also summarized in Algorithm 1.

Complexity requirements: it is not difficult to show that the computational complexity involved for implementing the Rao test at the FC is $\mathcal{O}(K\,p + p^2)$, i.e. a linear scaling in the number of sensors, and a quadratic scaling in the size of the unknown vector $\boldsymbol{\theta}$. This contrasts with the GLRT complexity, whose grid-based implementation scales as $\mathcal{O}(K\,N_\theta^p)$, where N_θ is the size of the per-dimension quantization grid applied to the vector $\boldsymbol{\theta}$. This incurs in a linear scaling in the number of sensors, but an exponential scaling in the size of the unknown vector. We recall that the above complexity measures have been calculated under the assumptions that all the pre-computations not depending on

Fusion	Complexity	
Rule	for each $\boldsymbol{y}$	change of $\{\boldsymbol{c}_k, \tau_k\}_{k=1}^K$
GLR	$\mathcal{O}(KN_\theta^p)$	$\mathcal{O}\left(K(m^2 + mN_\theta^p)\right)$
Rao	$\mathcal{O}(Kp + p^2)$	$\mathcal{O}\left(K(m^2 + mp + p^2) + p^3\right)$

$\boldsymbol{y}$ have been already performed and stored in memory at the FC (e.g. $\boldsymbol{I}^{-1}(\boldsymbol{\theta}_0)$ for Rao test). Still, for completeness, the above complexity terms are also reported (separately) since they are needed upon a change of the pairs $\{\boldsymbol{c}_k, \tau_k\}_{k=1}^K$. The overall summary of complexity for both the fusion rules is reported in Table II.

In what follows, we discuss how the general Rao statistic obtained herein specializes in the (i) SL and (ii) VL models, respectively. Still, we highlight the appeal of Rao test (closed-form) implementation even in the general non-linear case, as only the terms $\boldsymbol{g}_k(\boldsymbol{\theta})$ and $\boldsymbol{J}_k(\boldsymbol{\theta})$ (evaluated at $\boldsymbol{\theta}_0$) are required.

1) Rao Fusion Rule for SL Model: In case the measurement model corresponds to the SL model described in Eq. (2), the Rao statistic is simplified as follows. Specifically, we obtain $\boldsymbol{\delta}(\boldsymbol{y};\boldsymbol{\theta}) \to \delta(\boldsymbol{y};\theta)$ and $\boldsymbol{I}(\boldsymbol{\theta}) \to I(\theta)$ (i.e. both the score function and the FIM become scalar-valued, since θ is scalar), with the corresponding *simplified forms:*

$$\delta(\boldsymbol{y};\theta) = \sum_{k=1}^K q_k(\theta)[y_k - \psi_k(\theta)] h_k c_k \qquad (16)$$

$$I(\theta) = \sum_{k=1}^K q_k(\theta)^2 \psi_k(\theta)[1 - \psi_k(\theta)] h_k^2 c_k^2 \qquad (17)$$

Similarly, the auxiliary quantities employed in Eqs. (16) and (17) are equal to $\psi_k(\theta) = \mathcal{Q}(\frac{\tau_k - c_k h_k \theta}{|c_k|\sigma_k})(1 - 2\epsilon_k) + \epsilon_k$ and $q_k(\theta) = [\zeta_k p_{v_k}(\tau_k - c_k h_k \theta)]/[\psi_k(\theta)(1 - \psi_k(\theta))]$, respectively. Finally, the substitution $\theta = \theta_0 = 0$ in Eqs. (16) and (17) provides the explicit Rao statistic for SL model.

We recall that a fusion rule based on the Rao test for the SL model case (Eq. (2)) has been studied in [38]. Similarly, the GLRT for the same measurement model has been tackled in [6].

2) Rao Fusion Rule for VL Model: Differently, when the sensing phase adheres to the VL measurement model described in Eq. (3), the following simplified expressions hold, as the VL model is a special instance of the general case when $\boldsymbol{g}_k(\boldsymbol{\theta}) = \boldsymbol{H}_k\boldsymbol{\theta}$ and $\boldsymbol{\theta}_0 = \boldsymbol{0}$:

$$\boldsymbol{\delta}(\boldsymbol{y};\boldsymbol{\theta}) = \sum_{k=1}^K q_k(\boldsymbol{\theta})[y_k - \psi_k(\boldsymbol{\theta})] \boldsymbol{z}_k \qquad (18)$$

$$\boldsymbol{I}(\boldsymbol{\theta}) = \sum_{k=1}^K q_k(\boldsymbol{\theta})^2 \psi_k(\boldsymbol{\theta})[1 - \psi_k(\boldsymbol{\theta})] \boldsymbol{z}_k \boldsymbol{z}_k^T \qquad (19)$$

where we have defined $\boldsymbol{z}_k \triangleq \boldsymbol{H}_k^T \boldsymbol{c}_k$. Similarly, the auxiliary quantities employed in Eqs. (18) and (19) equal to $\psi_k(\boldsymbol{\theta}) = \mathcal{Q}(\frac{\tau_k - \boldsymbol{z}_k^T \boldsymbol{\theta}}{\sqrt{\boldsymbol{c}_k^T \boldsymbol{\Sigma}_k \boldsymbol{c}_k}})(1 - 2\epsilon_k) + \epsilon_k$ and $q_k(\boldsymbol{\theta}) = [\zeta_k p_{v_k}(\tau_k - \boldsymbol{z}_k^T \boldsymbol{\theta})]/[\psi_k(\boldsymbol{\theta})(1 - \psi_k(\boldsymbol{\theta}))]$, respectively. Finally, the substitution $\boldsymbol{\theta} = \boldsymbol{\theta}_0 = \boldsymbol{0}_p$ in Eqs. (18) and (19) provides the explicit Rao statistic for VL model.

From the general Rao test expression in Eq. (15), we observe that its implementation (and, consequently, its performance) depends on the specific choice of the quantizer parameters $(\tau_k, \boldsymbol{c}_k)$, $k = 1, \ldots, K$. Accordingly, these can be *designed* to *optimize* performance.

IV. DESIGN OF SENSORS' PARAMETERS

The focus of this section is the design of the parameters for the hyperplane-based sensors quantizers considered in this work. Specifically, we first asymptotically characterize the performance of both GLRT and Rao test for the considered general model (Section IV-A). Then, based on the above characterization, we design thresholds (Section IV-B) and compression vectors (Section IV-C) for all the sensors.

A. Asymptotic Performance Characterization

We know from the classical hypothesis testing literature that the asymptotic performance, in weak-signal condition, of Rao test and GLRT is given by [23]:

$$\Lambda_R, \Lambda_G \overset{a}{\sim} \begin{cases} \chi_p^2 & \text{under } \mathcal{H}_0 \\ \chi_p'^2(\lambda) & \text{under } \mathcal{H}_1 \end{cases} \qquad (20)$$

where λ denotes the non-centrality parameter:

$$\lambda \triangleq (\boldsymbol{\theta}_1 - \boldsymbol{\theta}_0)^T \boldsymbol{I}(\boldsymbol{\theta}_0)(\boldsymbol{\theta}_1 - \boldsymbol{\theta}_0) \qquad (21)$$

with $\boldsymbol{\theta}_1$ being the true value under $\mathcal{H}_1$. Clearly, the performance of both Rao test and GLRT increases *monotonically* with λ. The explicit form for λ (readily obtained by exploiting FIM expression in Eq. (14)) is:

$$\lambda = \sum_{k=1}^K \Big\{ q_k(\boldsymbol{\theta}_0, \tau_k, \boldsymbol{c}_k)^2 \, \psi_k(\boldsymbol{\theta}_0, \tau_k, \boldsymbol{c}_k)$$
$$\times [1 - \psi_k(\boldsymbol{\theta}_0, \tau_k, \boldsymbol{c}_k)] \, \langle \boldsymbol{c}_k, \boldsymbol{J}_k(\boldsymbol{\theta}_0)(\boldsymbol{\theta}_1 - \boldsymbol{\theta}_0) \rangle^2 \Big\} \qquad (22)$$

with a slight abuse of notation for $q_k(\boldsymbol{\theta}, \tau_k, \boldsymbol{c}_k)$ and $\psi_k(\boldsymbol{\theta}, \tau_k, \boldsymbol{c}_k)$, to stress their dependence on $(\tau_k, \boldsymbol{c}_k)$. The above expression underlines dependence of detection performance with respect to the nodes' parameters– i.e. local thresholds (τ_k) and compression vectors ($\boldsymbol{c}_k$)– whose design is discussed in the sequel.

Before proceeding, we report for completeness the specialized forms of the non-centrality parameter λ in the cases of (i) SL and (ii) VL measurement models. Specifically, in the SL measurement model [5], [6], we have

$$\text{(SL)} \quad \lambda = \sum_{k=1}^K \Big\{ q_k(0, \tau_k, c_k)^2 \, \psi_k(0, \tau_k, c_k)$$
$$\times [1 - \psi_k(0, \tau_k, c_k)] \, c_k^2 h_k^2 \theta_1^2 \Big\} \qquad (23)$$

while in the VL measurement model, we obtain

$$(\textbf{VL}) \quad \lambda = \sum_{k=1}^{K} \Big\{ q_k \left(\mathbf{0}_p, \tau_k, \boldsymbol{c}_k \right)^2 \, \psi_k(\mathbf{0}_p, \tau_k, \boldsymbol{c}_k)$$
$$\times \left[1 - \psi_k(\mathbf{0}_p, \tau_k, \boldsymbol{c}_k) \right] \langle \boldsymbol{c}_k, \, \boldsymbol{H}_k \boldsymbol{\theta}_1 \rangle^2 \Big\} \quad (24)$$

The objective of next subsections is to design thresholds τ_k and compression vectors $\boldsymbol{c}_k$ so as to optimize the asymptotic performance of GLRT and Rao test, that is:

$$\{\tau_k^\star, \boldsymbol{c}_k^\star\}_{k=1}^{K} = \underset{\{\boldsymbol{c}_k, \tau_k\}_{k=1}^{K}}{\arg\max} \, \lambda \left(\{\tau_k, \boldsymbol{c}_k\}_{k=1}^{K} \right) \quad (25)$$

To this end, we rewrite the non-centrality parameter objective in Eq. (22) as follows:

$$\lambda \left(\{\tau_k, \, \boldsymbol{c}_k\}_{k=1}^{K} \right) = \sum_{k=1}^{K} \kappa_k \left(\tau_k, \boldsymbol{c}_k \right) \, \beta_k(\boldsymbol{c}_k) \quad (26)$$

where we have defined $\kappa_k(\tau_k, \boldsymbol{c}_k) \triangleq q_k(\boldsymbol{\theta}_0, \tau_k, \boldsymbol{c}_k)^2 \psi_k(\boldsymbol{\theta}_0, \tau_k, \boldsymbol{c}_k) \left[1 - \psi_k(\boldsymbol{\theta}_0, \tau_k, \boldsymbol{c}_k) \right]$ and $\beta_k(\boldsymbol{c}_k) \triangleq \langle \boldsymbol{c}_k, \boldsymbol{J}_k(\boldsymbol{\theta}_0)(\boldsymbol{\theta}_1 - \boldsymbol{\theta}_0) \rangle^2$, respectively.

Remarkably, the additive form of the non-centrality parameter λ allows each sensor to be optimized *independently*. Additionally, all the involved terms are *non-negative*. Accordingly, we first obtain each quantizer threshold by maximizing the per-sensor contribution $\kappa_k(\tau_k, \boldsymbol{c}_k)$ so as to obtain an optimized $\tau_k^\star(\boldsymbol{c}_k)$ (i.e. being function of the compression vectors). Once obtained the $\tau_k^\star(\boldsymbol{c}_k)$, subsequently, we will focus on each $\boldsymbol{c}_k$ design.

B. Design of Local Quantizers' Thresholds $\{\tau_k\}_{k=1}^{K}$

As previously discussed, we concentrate herein on optimized local thresholds τ_k. More specifically, each τ_k is obtained as the solution of the following optimization:

$$\tau_k^\star(\boldsymbol{c}_k) \triangleq \arg\max_{\tau_k} \kappa_k(\tau_k, \boldsymbol{c}_k). \quad (27)$$

To obtain a solution for the aforementioned problem, we first rewrite $\kappa_k(\tau_k, \boldsymbol{c}_k)$ exploiting the definitions of $\psi_k(\boldsymbol{\theta}_0, \tau_k, \boldsymbol{c}_k)$ and $q_k(\boldsymbol{\theta}_0, \tau_k, \boldsymbol{c}_k)$ (Eqs. (7) and (13), respectively). Hence, after some manipulations, we obtain:

$$\kappa_k(\tau_k, \boldsymbol{c}_k) = \frac{\zeta_k^2 \, p_{v_k}^2 \left(\tau_k - \boldsymbol{c}_k^T \boldsymbol{g}_k(\boldsymbol{\theta}_0) \right)}{\psi_k(\boldsymbol{\theta}_0, \tau_k, \boldsymbol{c}_k) \left[1 - \psi_k(\boldsymbol{\theta}_0, \tau_k, \boldsymbol{c}_k) \right]}$$
$$= \frac{p_{v_k}^2 \left(\tau_k - \boldsymbol{c}_k^T \boldsymbol{g}_k(\boldsymbol{\theta}_0) \right)}{\mathcal{Q}\left(\frac{\tau_k - \boldsymbol{c}_k^T \boldsymbol{g}_k(\boldsymbol{\theta}_0)}{\sqrt{\boldsymbol{c}_k^T \boldsymbol{\Sigma}_k \boldsymbol{c}_k}} \right) \left[1 - \mathcal{Q}\left(\frac{\tau_k - \boldsymbol{c}_k^T \boldsymbol{g}_k(\boldsymbol{\theta}_0)}{\sqrt{\boldsymbol{c}_k^T \boldsymbol{\Sigma}_k \boldsymbol{c}_k}} \right) \right] + \Delta_k} \quad (28)$$

where $\Delta_k \triangleq [\epsilon_k(1 - \epsilon_k)]/(1 - 2\epsilon_k)^2$. Then, since $v_k \sim \mathcal{N}(0, \boldsymbol{c}_k^T \boldsymbol{\Sigma}_k \boldsymbol{c}_k)$, it follows from known results in the literature of (scalar) quantized estimation and detection [25], [38], [39] that $\tau_k^\star(\boldsymbol{c}_k) = \boldsymbol{c}_k^T \boldsymbol{g}_k(\boldsymbol{\theta}_0)$ corresponds to the optimum threshold. This property also applies *independently on the specific value of the BEP* ϵ_k.

Substituting the optimal value $\tau_k^\star(\boldsymbol{c}_k)$ within Eq. (28) provides the (threshold-)optimized objective $\kappa_k(\tau_k^\star, \boldsymbol{c}_k)$, whose explicit

expression is:

$$\kappa_k(\tau_k^\star, \boldsymbol{c}_k) = \frac{p_{v_k}^2(0)}{\mathcal{Q}(0) \left[1 - \mathcal{Q}(0) \right] + \Delta_k} \quad (29)$$

Furthermore, by observing that $\mathcal{Q}(0) = 1/2$ and $p_{v_k}(0) = 1/\sqrt{2\pi \boldsymbol{c}_k^T \boldsymbol{\Sigma}_k \boldsymbol{c}_k}$, respectively, the function $\kappa_k(\tau_k^\star, \boldsymbol{c}_k)$ can be simplified as:

$$\kappa_k(\tau_k^\star, \boldsymbol{c}_k) = \frac{2 \, \zeta_k^2}{\pi \, \left(\boldsymbol{c}_k^T \boldsymbol{\Sigma}_k \boldsymbol{c}_k \right)} \quad (30)$$

We conclude the section with a mention on SL and VL measurement models. First, since in scalar and vector cases $\theta_0 = 0$ and $\boldsymbol{\theta}_0 = \mathbf{0}_p$ hold, respectively, it is not difficult to show that such result implies $\tau_k^\star = 0$ in both SL (thus confirming the results in [5], [6]) and VL measurement models. The optimized objective in Eq. (30) then specializes into $\kappa_k(\tau_k^\star, c_k) = \frac{2 \zeta_k^2}{\pi c_k^2 \sigma_k^2}$ for the SL model, while retains the same form as Eq. (30) for the VL model.

C. Design of Compression Vectors $\{\boldsymbol{c}_k\}_{k=1}^{K}$

Once the thresholds τ_k have been optimized, the non-centrality parameter $\lambda(\cdot)$ becomes:

$$\lambda \left(\{\tau_k^\star, \boldsymbol{c}_k\}_{k=1}^{K} \right) = \sum_{k=1}^{K} \kappa_k \left(\tau_k^\star, \boldsymbol{c}_k \right) \, \beta_k(\boldsymbol{c}_k) \quad (31)$$

$$= \sum_{k=1}^{K} \frac{2 \, \zeta_k^2}{\pi} \frac{\boldsymbol{c}_k^T \boldsymbol{J}_k(\boldsymbol{\theta}_0)(\boldsymbol{\theta}_1 - \boldsymbol{\theta}_0)(\boldsymbol{\theta}_1 - \boldsymbol{\theta}_0)^T \boldsymbol{J}_k(\boldsymbol{\theta}_0) \, \boldsymbol{c}_k}{\boldsymbol{c}_k^T \boldsymbol{\Sigma}_k \boldsymbol{c}_k} \quad (32)$$

The τ_k-optimal non-centrality parameter in Eq. (22) specializes, for the SL model, in:

$$(\textbf{SL}) \quad \lambda \left(\{\tau_k^\star, c_k\}_{k=1}^{K} \right) = \frac{2}{\pi} \sum_{k=1}^{K} \zeta_k^2 \, \frac{h_k^2 \, \theta_1^2}{\sigma_k^2} \quad (33)$$

From the above equation, it is apparent that a scalar scaling of the measurement *would not alter asymptotic performance*. On the other hand, in the case of a VL model, τ_k-optimal non-centrality parameter simplifies to

$$(\textbf{VL}) \quad \lambda \left(\{\tau_k^\star, \boldsymbol{c}_k\}_{k=1}^{K} \right) = \frac{2}{\pi} \sum_{k=1}^{K} \zeta_k^2 \, \frac{\boldsymbol{c}_k^T \, \boldsymbol{H}_k \, \boldsymbol{\theta}_1 \boldsymbol{\theta}_1^T \, \boldsymbol{H}_k^T \, \boldsymbol{c}_k}{\boldsymbol{c}_k^T \boldsymbol{\Sigma}_k \boldsymbol{c}_k} \quad (34)$$

Thus, in the general case, each optimal compression vector $\boldsymbol{c}_k^\star$ would be the solution of the following optimization problem (discarding irrelevant terms)

$$\max_{\boldsymbol{c}_k} \frac{\langle \boldsymbol{c}_k, \boldsymbol{J}_k(\boldsymbol{\theta}_0) \, (\boldsymbol{\theta}_1 - \boldsymbol{\theta}_0) \rangle^2}{\boldsymbol{c}_k^T \boldsymbol{\Sigma}_k \boldsymbol{c}_k} . \quad (35)$$

After defining $\bar{\boldsymbol{c}}_k \triangleq \boldsymbol{\Sigma}_k^{1/2} \boldsymbol{c}_k$ the above optimization can be rewritten as:

$$\max_{\bar{\boldsymbol{c}}_k} \frac{\left\langle \bar{\boldsymbol{c}}_k, \, \boldsymbol{\Sigma}_k^{-1/2} \boldsymbol{J}_k(\boldsymbol{\theta}_0) \, (\boldsymbol{\theta}_1 - \boldsymbol{\theta}_0) \right\rangle^2}{\bar{\boldsymbol{c}}_k^T \bar{\boldsymbol{c}}_k} . \quad (36)$$

Then, using *Cauchy-Schwarz* inequality, we have:

$$\frac{\left\langle \bar{c}_k, \, \Sigma_k^{-1/2} J_k(\theta_0)(\theta_1 - \theta_0) \right\rangle^2}{\bar{c}_k^T \bar{c}_k}$$

$$\leq \left\| \Sigma_k^{-1/2} J_k(\theta_0)(\theta_1 - \theta_0) \right\|^2. \tag{37}$$

The equality in (37) is achieved when $\bar{c}_k = \bar{c}_k^\star \triangleq \alpha \Sigma_k^{-1/2} J_k(\theta_0)(\theta_1 - \theta_0)$, with $\alpha \in \mathbb{R} \setminus \{0\}$.

Finally, (i) substituting back the expression of $\bar{c}_k^\star$ into c_k and (ii) choosing c_k such that $\|c_k\|^2 = 1$, provide the optimal solution in explicit form:

$$c_k^\star = \frac{\Sigma_k^{-1} J_k(\theta_0)(\theta_1 - \theta_0)}{\left\| \Sigma_k^{-1} J_k(\theta_0)(\theta_1 - \theta_0) \right\|} \tag{38}$$

Unfortunately, since the true value of θ_1 is *not known* at the FC, the optimal compression vector $c_k^\star$ *cannot be implemented*.[1] We recall that this is also the case for the (simpler) VL measurement model, whose corresponding explicit solution is $c_k^\star = \Sigma_k^{-1} H_k \theta_1 / \| \Sigma_k^{-1} H_k \theta_1 \|$. Therefore, the need for *sub-optimal design approaches* arises. Herein, *four* different heuristic alternatives are explored, described hereinafter.

Random precoding (RND) corresponds to the naivest precoding approach, as adopted in [33] for decentralized detection in the no-quantization case. Specifically, the compression vectors are chosen such that $c_k \sim \mathcal{N}(0_m, I_m)$ and then normalized as $c_k / \|c_k\|$.

Uniform precoding (UNF) hypothesizes that the vector θ_1 deviates from the nominal θ_0 with an equal-sized contribution on each component (i.e. $\theta_1 = \theta_0 + 1_p$), namely

$$c_k = \frac{\Sigma_k^{-1} J_k(\theta_0) 1_p}{\left\| \Sigma_k^{-1} J_k(\theta_0) 1_p \right\|} \tag{39}$$

Random subspace precoding (RSP) consists in considering the singular value decomposition of the matrix $\Psi \triangleq \Sigma_k^{-1} J_k(\theta_0)$, namely $\Psi = U_\Psi \Lambda_\Psi V_\Psi^T$, and randomly sampling one of the columns of U_Ψ. By doing so, the RSP compression vector c_k will be guaranteed to lie within the *same subspace* as the optimal $c_k^\star$.

Top(-direction) subspace precoding (TSP) similarly considers the singular value decomposition of the matrix Ψ, namely $\Psi = U_\Psi \Lambda_\Psi V_\Psi^T$, but rather uses the column of U_Ψ associated to the *highest singular value*. In this way, the compression vector will be guaranteed to lie within the same subspace as the optimal $c_k^\star$ and be aligned along the direction with the highest sensitivity with respect to deviations of $(\theta_1 - \theta_0)$.

Remarks: clearly, the RND approach does not capitalize any knowledge of the sensing subspace, while the sensing model is partially capitalized by UNF precoding. Conversely, RSP and TSP are likely to better capitalize the *whole* subspace information deriving from the sensing model. Finally, we stress that we do not consider sign-assisted precoding [33] in our

---

[1] We recall that, in case of simpler (linear) g_k mapping and analog transmission, the ML estimate of θ_1 could be obtained in closed form at the FC. Hence, when multiple samples are collected by the WSN, the running estimate of θ_1 could be exploited to implement Eq. (38) at FC side. However, this procedure would require the additional (per-sample) feedback from the FC to the sensors to transmit the updated c_k [40].

Algorithm 2: *Optimized* quantizer processing at kth sensor.

> **Sensing Model Params:** $\{\Sigma_k, g_k(\theta_0), J_k(\theta_0)\}$
> **Input:** vector measurement x_k;
> **Output:** the bit b_k sent to the FC.
> 1: Select c_k according to the heuristic selected (e.g. RND);
> 2: Set $\tau_k^\star(c_k) = c_k^T g_k(\theta_0)$;
> 3: Quantize the measurement as $b_k = u(c_k^T x_k - \tau_k^\star)$;

Algorithm 3: *Optimized* parameters computation at the FC.

> **Input:** $\{\Sigma_k, g_k(\theta_0), J_k(\theta_0)\}_{k=1}^K$
> **Output:** heuristic compression vectors $c_1, \ldots, c_K$; opt. quantization thresholds $\tau_1^\star, \ldots, \tau_K^\star$;
> 1: **for** $k = 1, \ldots, K$ **do**
> 2:   Select c_k according to the same sensor heuristic;
> 3:   Set $\tau_k^\star(c_k) = c_k^T g_k(\theta_0)$;
> 4: **end for**

---

analysis, which leverages the clairvoyant knowledge of the sign of $(\theta_1 - \theta_0)$ but works effectively only under the condition $\Psi = \Sigma_k^{-1} J_k(\theta_0) = I_p$. Indeed, in general ($\Psi \neq I_p$), the sign information on $(\theta_1 - \theta_0)$ does not bring any useful information about the sign of c_k.

D. Implementation Aspects of the Proposed Design

In this section, we discuss how the previously-derived optimized quantizer design can be implemented in practice. First of all, we highlight that *all* the four compression heuristics considered have a sole per-sensor dependence, namely c_k depends only on the parameters associated to sensor k. Additionally, each compression vector c_k does not depend on the specific BEP condition, i.e. ϵ_k. Such properties originate from the peculiar form of the optimal $c_k^\star$, see Eq. (38). Such remarkable properties also apply to the optimized thresholds, because of the functional form $\tau_k^\star(c_k) = c_k^T g_k(\theta_0)$. Accordingly, each pair $(c_k, \tau_k^\star)$ can be calculated by both the kth sensor and the FC, *without additional information exchange*. The only pre-requisite is that kth sensor should know the statistical characterization pertaining to its sensing model (namely, $\{\Sigma_k, g_k(\theta_0), J_k(\theta_0)\}$), whereas the statistical characterization pertaining to the sensing models of all the sensors (namely, $\{\Sigma_k, g_k(\theta_0), J_k(\theta_0)\}_{k=1}^K$) should be available at the FC. The procedures for (optimized) quantizer processing at the kth sensor and the computation of all sensors' quantizers parameters at the FC are reported in Algos. 2 and 3, respectively. Clearly, a corresponding information exchange (with additional overhead) between the sensors and the FC is required only upon a (statistical) change of the sensing model.

Furthermore, we observe that for RND and RSP precoding additional coordination between the sensors and the FC is required, since they rely on a random generation process for sampling the unscaled c_k and the chosen column of U_Ψ, respectively (cf. Section IV-C). However, in the above case, it only suffices that the FC will have a twin pseudo-random generator (with the same initial seed) as each sensor.

V. ENABLING MULTI-BIT QUANTIZATION

In this section, we extend the findings obtained in the previous sections to the multi-bit quantizer. More specifically, hereinafter we assume that kth sensor quantizes its measurement vector into $m_k \leq m$ bits, whose expressions are as follows [35]:

$$b_{k,i} \triangleq u\left(\boldsymbol{c}_{k,i}^T \boldsymbol{x}_k - \tau_{k,i}\right) \quad i = 1, \ldots, m_k \quad (40)$$

In the above equation $b_{k,i}$ denotes the ith bit obtained from quantization of measurement vector $\boldsymbol{x}_k$ via a hyperplane-based quantizer having $\boldsymbol{c}_{k,i}$ and $\tau_{k,i}$ as the corresponding compression vector and quantization threshold, respectively. The above set of quantizers can be also rewritten in the compact form $\boldsymbol{b}_k = \boldsymbol{u}(\boldsymbol{C}_k^T \boldsymbol{x}_k - \boldsymbol{\tau}_k)$, where $\boldsymbol{b}_k \triangleq [b_{k,1} \ldots b_{k,m_k}]^T \in \{0,1\}^{m_k}$, $\boldsymbol{C}_k \triangleq [\boldsymbol{c}_{k,1} \cdots \boldsymbol{c}_{k,m_k}] \in \mathbb{R}^{m \times m_k}$, $\boldsymbol{\tau}_k \triangleq [\tau_{k,1} \cdots \tau_{k,m_k}] \in \mathbb{R}^{m_k}$, and by interpreting the (vector) unit-step function $\boldsymbol{u}(\cdot)$ in an elementwise fashion.

For simplicity, we will enforce *statistical independence* among the bits of the same sensor. For $b_{k,i}$ and $b_{k,j}$ to be independent, it suffices $\boldsymbol{c}_{k,i}^T \boldsymbol{x}_k$ and $\boldsymbol{c}_{k,j}^T \boldsymbol{x}_k$ to be uncorrelated, since the noise vector is Gaussian-distributed. In other terms, the *sufficient condition* is written in a compact form as:

$$\mathbb{E}\left(\boldsymbol{C}_k^T \boldsymbol{w}_k \boldsymbol{w}_k^T \boldsymbol{C}_k\right) = \boldsymbol{C}_k^T \boldsymbol{\Sigma}_k \boldsymbol{C}_k = c\, \boldsymbol{I}_{m_k} \quad (41)$$

where c is a constant, herein chosen to unity without loss of generality. The above condition can be met by choosing the compression matrix for kth sensor as $\boldsymbol{C}_k = \boldsymbol{\Sigma}_k^{-1/2} \boldsymbol{U}_k$ where $\boldsymbol{U}_k \triangleq [\boldsymbol{v}_{k,1} \cdots \boldsymbol{v}_{k,m_k}]$ denotes a slice of a unitary basis, that is $\boldsymbol{U}_k^\dagger \boldsymbol{U}_k = \boldsymbol{I}_{m_k}$. We highlight that the above choice corresponds to enforcing a lattice-type structure to the vector quantizers considered herein.

Remarks: for the multi-bit case, we make the assumption $\sum_{k=1}^{K} m_k > p$, i.e. there are enough independent WSN measurements to (implicitly) estimate the unknown vector $\boldsymbol{\theta}$.

Before proceeding, we denote the received vector from kth sensor by $\boldsymbol{y}_k \triangleq [y_{k,1} \ldots y_{k,m_k}]^T$ with the same communication channel impact discussed in Eq. (5). Accordingly, the overall transmitted and received vectors are defined as $\boldsymbol{b} \triangleq [\boldsymbol{b}_1^T \ldots \boldsymbol{b}_K^T]^T$ and $\boldsymbol{y} \triangleq [\boldsymbol{y}_1^T \ldots \boldsymbol{y}_K^T]^T$ (both $\in \{0,1\}^{\sum_{k=1}^{K} m_k}$), respectively.

In what follows, we first derive both the fusion rules for the multi-bit case with reference to the non-linear sensing model in Eq. (1) (Section V-A). Secondly, we provide their corresponding asymptotic characterization in the above case (Section V-B). Finally, we deal with the design of multi-bit quantizers (Section V-C).

A. Multi-Bit Fusion Rules

We first focus on obtaining the likelihood function $P_{\mathrm{mb}}(\boldsymbol{y}; \boldsymbol{\theta})$ for the multi-bit quantization case. It is not difficult to show that, in such case, the explicit expression generalizes as follows:

$$P_{\mathrm{mb}}(\boldsymbol{y}; \boldsymbol{\theta}) = \prod_{k=1}^{K} \prod_{i=1}^{m_k} [\psi_{k,i}(\boldsymbol{\theta})]^{y_{k,i}} [1 - \psi_{k,i}(\boldsymbol{\theta})]^{(1-y_{k,i})} \quad (42)$$

where

$$\psi_{k,i}(\boldsymbol{\theta}) = \mathcal{Q}\left(\tau_{k,i} - \left[\boldsymbol{\Sigma}_k^{-1/2} \boldsymbol{v}_{k,i}\right]^T \boldsymbol{g}_k(\boldsymbol{\theta})\right)(1 - 2\epsilon_k) + \epsilon_k \quad (43)$$

TABLE III
COMPUTATIONAL COMPLEXITY OF MULTI-BIT FUSION RULES: m_k IS THE NUMBER OF BITS SENT FROM kTH SENSOR TO THE FC; m IS THE SIZE OF THE MEASUREMENT SPACE; p IS THE SIZE OF THE PARAMETER VECTOR; N_θ DENOTES THE NUMBER OF BINS USED FOR DISCRETIZING EACH DIMENSION OF THE VECTOR $\boldsymbol{\theta}$.

Fusion Rule	Complexity	
	for each y	change of $\{c_k, \tau_k\}_{k=1}^{K}$
GLR	$\mathcal{O}(\sum_{k=1}^{K} m_k\, N_\theta^p)$	$\mathcal{O}(\sum_{k=1}^{K} m_k\, (m^2 + m N_\theta^p))$
Rao	$\mathcal{O}(\sum_{k=1}^{K} m_k p + p^2)$	$\mathcal{O}(\sum_{k=1}^{K} m_k(m^2 + mp + p^2) + p^3)$

The above result follows from $v_{k,i} \triangleq (\boldsymbol{\Sigma}_k^{-1/2} \boldsymbol{v}_{k,i})^T \boldsymbol{w}_k$ being a zero-mean unit-variance Gaussian RV. First, we observe that the GLR statistic can be obtained by substituting Eq. (42) into the general expression provided in Eq. (9). Hence, it is not reported for brevity. Clearly, the GLR statistic retains the same difficulties as the one-bit case.

On the other hand, we show in what follows that Rao test *admits a closed-form* even in this setup. This result is accomplished by capitalizing the explicit expressions of the score vector and the FIM, which are reported in the following two propositions.

Proposition 3: The closed-form multi-bit score vector is:

$$\boldsymbol{\delta}_{\mathrm{mb}}(\boldsymbol{y}; \boldsymbol{\theta}) =$$

$$\sum_{k=1}^{K} \sum_{i=1}^{m_k} \left\{ q_{k,i}(\boldsymbol{\theta})\left[y_{k,i} - \psi_{k,i}(\boldsymbol{\theta})\right] \boldsymbol{J}_k^T(\boldsymbol{\theta}) \boldsymbol{\Sigma}_k^{-1/2} \boldsymbol{v}_{k,i} \right\} \quad (44)$$

where

$$q_{k,i}(\boldsymbol{\theta}) \triangleq \frac{\zeta_k\, p_{v_{k,i}}\left(\tau_{k,i} - \left[\boldsymbol{\Sigma}_k^{-1/2} \boldsymbol{v}_{k,i}\right]^T \boldsymbol{g}_k(\boldsymbol{\theta})\right)}{\psi_{k,i}(\boldsymbol{\theta})\left(1 - \psi_{k,i}(\boldsymbol{\theta})\right)} \quad (45)$$

Proof: The proof is similar to that contained in Appendix A and thus not reported for brevity.

Proposition 4: The explicit form of the FIM with multi-bit sensors:

$$\boldsymbol{I}_{\mathrm{mb}}(\boldsymbol{\theta}) = \sum_{k=1}^{K} \sum_{i=1}^{m_k} \left\{ q_{k,i}(\boldsymbol{\theta})^2\, \psi_{k,i}(\boldsymbol{\theta})\left[1 - \psi_{k,i}(\boldsymbol{\theta})\right] \right.$$

$$\left. \times\, \boldsymbol{J}_k^T(\boldsymbol{\theta})\, \boldsymbol{\Sigma}_k^{-1/2} \boldsymbol{v}_{k,i} \boldsymbol{v}_{k,i}^T \boldsymbol{\Sigma}_k^{-1/2} \boldsymbol{J}_k(\boldsymbol{\theta}) \right\} \quad (46)$$

Proof: The derivation follows on from the proof contained in Appendix B. Hence, it is omitted for brevity.

Complexity requirements: The computational complexity of multi-bit Rao test is $\mathcal{O}(\sum_{k=1}^{K} m_k\, p + p^2)$, i.e. a linear scaling in the number of sensors and bit resolution, and a quadratic scaling in the size of the unknown vector $\boldsymbol{\theta}$. Conversely, GLRT complexity (based on grid-implementation) scales as $\mathcal{O}((\sum_{k=1}^{K} m_k)\, N_\theta^p)$, where N_θ is the size of the per-dimension quantization grid applied to the vector $\boldsymbol{\theta}$. This incurs in a linear scaling in the number of sensors and their bit resolution, but an exponential scaling in the size of the unknown vector. The complexity summary for both the multi-bit fusion rules is reported in Table III. As in the one-bit case, the aforementioned table reports also the corresponding complexity measures associated to pre-computations and needed upon a change of the pairs $\{\{\boldsymbol{c}_{k,i}, \tau_{k,i}\}_{i=1}^{m_k}\}_{k=1}^{K}$.

We now report the specialization of the multi-bit Rao fusion rule to the VL model. Indeed, we recall that, for the SL model, there is only one measurement dimension ($m = 1$). Nonetheless, we recall the general appeal of multi-bit Rao test (closed-form) implementation in the general *non-linear* case, as no additional terms are required even when varying the bit resolution (e.g. $g_k(\theta)$ and $J_k(\theta)$, evaluated at θ_0, are solely required also in this case).

A. Multi-bit Rao Fusion Rule for VL model: For the VL measurement model in Eq. (3), the score vector and the FIM reduce to

$$\delta_{\mathrm{mb}}(y;\theta) = \sum_{k=1}^{K}\sum_{i=1}^{m_k}\left\{ q_{k,i}(\theta)\left[y_{k,i}-\psi_{k,i}(\theta)\right]H_k^T \Sigma_k^{-1/2}v_{k,i}\right\} \tag{47}$$

and

$$I_{\mathrm{mb}}(\theta) = \sum_{k=1}^{K}\sum_{i=1}^{m_k}\left\{ q_{k,i}(\theta)^2\,\psi_{k,i}(\theta)\left[1-\psi_{k,i}(\theta)\right] \right.$$
$$\left. \times\; H_k^T\Sigma_k^{-1/2}v_{k,i}v_{k,i}^T\Sigma_k^{-1/2}H_k\right\} \tag{48}$$

respectively. Differently, $\psi_{k,i}(\theta)$ simplifies into

$$\psi_{k,i}(\theta) = \mathcal{Q}\left(\tau_{k,i}-v_{k,i}^T\Sigma_k^{-1/2}H_k\theta\right)(1-2\epsilon_k)+\epsilon_k \tag{49}$$

Finally, the simplified $q_{k,i}(\theta)$ is evaluated as:

$$q_{k,i}(\theta) \triangleq \frac{\zeta_k\, p_{v_{k,i}}\left(\tau_{k,i}-v_{k,i}^T\Sigma_k^{-1/2}H_k\theta\right)}{\psi_{k,i}(\theta)\left(1-\psi_{k,i}(\theta)\right)} \tag{50}$$

B. Asymptotic Characterization of Multi-Bit Fusion Rules

Clearly, GLRT and Rao test retain the same asymptotic performance reported in Eq. (20), with the (multi-bit) non-centrality parameter λ_{mb} now given by:[2]

$$\lambda_{\mathrm{mb}} = \sum_{k=1}^{K}\sum_{i=1}^{m_k}\left\{ q_{k,i}(\theta_0,\tau_{k,i},v_{k,i})^2\,\psi_{k,i}(\theta_0,\tau_{k,i},v_{k,i})\right.$$
$$\left.\times[1-\psi_{k,i}(\theta_0,\tau_{k,i},v_{k,i})]\left\langle v_{k,i},\Sigma_k^{-1/2}J_k(\theta_0)(\theta_1-\theta_0)\right\rangle^2\right\} \tag{51}$$

Generalizing the one-bit case, detection performance now depends on $2\,m_k$ different parameters per-node, i.e. the local thresholds ($\tau_{k,i}$, $i=1,\ldots,m_k$) and the compression vectors ($v_{k,i}$, $i=1,\ldots,m_k$). Their proposed design is reported hereinafter. Finally, we observe that for the special VL measurement model, the explicit form of λ_{mb} is obtained (i) by exploiting Eqs. (49) and (50) into (51) and (ii) by replacing $J_k(\theta_0)(\theta_1-\theta_0)$ with $H_k\theta_1$.

The objective of next subsection is to design thresholds $\tau_{k,i}$ and (intra-sensor orthogonal) compression vectors $v_{k,i}$ so as to optimize the non-centrality parameter λ_{mb} (monotonically

related to the asymptotic performance of GLRT and Rao test), that is:

$$\{\tau_k^\star,U_k^\star\}_{k=1}^{K} = \operatorname*{arg\,max}_{\{\tau_k,U_k\}_{k=1}^{K}}\lambda_{\mathrm{mb}}\left(\{\tau_k,U_k\}_{k=1}^{K}\right) \tag{52}$$

To exploit the structural properties of the non-centrality parameter, the objective in Eq. (51) is rewritten, *analogously to one-bit case*, as

$$\lambda_{\mathrm{mb}}\left(\{\tau_k,U_k\}_{k=1}^{K}\right) = \sum_{k=1}^{K}\sum_{i=1}^{m_k}\kappa_{k,i}(\tau_{k,i},v_{k,i})\,\beta_{k,i}(v_{k,i}) \tag{53}$$

where the definitions $\kappa_{k,i}(\tau_{k,i},v_{k,i}) \triangleq q_{k,i}(\theta_0,\tau_{k,i},v_{k,i})^2\psi_{k,i}(\theta_0,\tau_{k,i},v_{k,i})\left[1-\psi_k(\theta_0,\tau_{k,i},v_{k,i})\right]$ and $\beta_{k,i}(v_{k,i}) \triangleq \left\langle v_{k,i},\Sigma_k^{-1/2}J_k(\theta_0)(\theta_1-\theta_0)\right\rangle^2$ have been employed.

The above form of the non-centrality parameter λ_{mb} allows (since all the involved terms are *non-negative*) first to obtain each quantizer threshold by maximizing the per-sensor per-bit contribution $\kappa_{k,i}(\tau_{k,i},v_{k,i})$ so as to obtain an optimized $\tau_{k,i}^\star(v_{k,i})$ (i.e. being function of the corresponding compression vector only). Once $\tau_{k,i}^\star(v_{k,i})$ is obtained, we will address the design of $v_{k,i}$'s.

C. Design of Sensors' Multi-Bit Quantizers

Hereinafter, based on the discussion in Section IV-B, the quantization thresholds $\tau_{k,i}$'s are given by $\tau_{k,i}^\star(v_{k,i}) \triangleq \operatorname*{arg\,max}_{\tau_{k,i}}\kappa_{k,i}(\tau_{k,i},v_{k,i})$. The above objective is expressed in closed-form as:

$$\kappa_{k,i}(\tau_{k,i},v_{k,i}) =$$
$$\frac{p_{v_{k,i}}^2\left(\tau_{k,i}-v_{k,i}^T\bar{g}_k(\theta_0)\right)}{\mathcal{Q}\left(\tau_{k,i}-v_{k,i}^T\bar{g}_k(\theta_0)\right)\left[1-\mathcal{Q}\left(\tau_{k,i}-v_{k,i}^T\bar{g}_k(\theta_0)\right)\right]+\Delta_k} \tag{54}$$

where $\bar{g}_k(\theta_0) \triangleq \Sigma_k^{-1/2}g_k(\theta_0)$. Then, exploiting similar results as one-bit case, it follows that $\tau_{k,i}^\star(v_{k,i}) = v_{k,i}^T\Sigma_k^{-1/2}g_k(\theta_0)$ corresponds to the optimum threshold. We remark that, even in the multi-bit case, the optimum threshold does not depend on the BEP value ϵ_k.

Substituting the optimal value $\tau_{k,i}^\star(v_{k,i})$ within Eq. (54) provides the (threshold-)optimized expression $\kappa_{k,i}(\tau_k^\star(v_{k,i}),v_{k,i})$, whose explicit form is:

$$\kappa_{k,i}(\tau_k^\star(v_{k,i}),v_{k,i}) = \frac{p_{v_{k,i}}^2(0)}{\mathcal{Q}(0)[1-\mathcal{Q}(0)]+\Delta_k} = \frac{2\zeta_k^2}{\pi} \tag{55}$$

Once we have optimized the thresholds $\tau_{k,i}$, the non-centrality parameter $\lambda_{\mathrm{mb}}(\cdot)$ assumes the following expression:

$$\lambda_{\mathrm{mb}}\left(\{\tau_k^\star(U_k),U_k\}_{k=1}^{K}\right)$$
$$= \sum_{k=1}^{K}\sum_{i=1}^{m_k}\kappa_{k,i}\left(\tau_{k,i}^\star(v_{k,i}),v_{k,i}\right)\beta_{k,i}(v_{k,i})$$
$$= \sum_{k=1}^{K}\frac{2\zeta_k^2}{\pi}\sum_{i=1}^{m_k}\left\langle v_{k,i},\Sigma_k^{-1/2}J_k(\theta_0)(\theta_1-\theta_0)\right\rangle^2 \tag{56}$$

Clearly, the unavailability of the true value of $\boldsymbol{\theta}_1$ leads to the same impracticability in the design of the optimal compression matrix $\boldsymbol{U}_k^\star$ as in the one-bit case. Correspondingly, these technical issues also hold for the (simpler) VL model.

Specifically, each sensor term $\sum_{i=1}^{m_k} \langle \boldsymbol{v}_{k,i}, \boldsymbol{\gamma}_k \rangle^2 = \boldsymbol{\gamma}_k^T (\boldsymbol{U}_k \boldsymbol{U}_k^T) \boldsymbol{\gamma}_k$ in Eq. (56) is a symmetric bilinear form, where $\boldsymbol{\gamma}_k \triangleq \boldsymbol{\Sigma}_k^{-1/2} \boldsymbol{J}_k(\boldsymbol{\theta}_0)(\boldsymbol{\theta}_1 - \boldsymbol{\theta}_0)$. By leveraging noteworthy properties of bilinear forms, it is known that such term is maximized when $\boldsymbol{\gamma}_k$ is aligned toward the eigenvector corresponding to the largest eigenvalue of $\boldsymbol{U}_k \boldsymbol{U}_k^T$. However, since $\boldsymbol{U}_k$ is a slice of a unitary basis, this is tantamount to achieve the displacement of $\boldsymbol{\gamma}_k$ within the subspace generated by $\boldsymbol{U}_k$ (as all the columns contribute equally in terms of energy). Accordingly, the (clairvoyant) matrix $\boldsymbol{U}_k^\star$ should be designed such that its generated subspace "covers" all the components of the vector $\boldsymbol{\gamma}_k$ (which depends on the *unknown* $\boldsymbol{\theta}_1$).

Accordingly, as in the case of one-bit quantization, the need for *sub-optimal design approaches* arises. Herein, *three* different heuristic alternatives are explored, described hereinafter and based on generalization of one-bit heuristics proposed in Section IV-C. We recall that these heuristics retain the same implementation requirements as the one-bit case in Section IV-D.

(Orthogonal) Random precoding (`RND`) corresponds to the naivest precoding approach, as adopted in [33] for decentralized detection in the no-quantization case. Specifically, the compression vectors are chosen such that $\boldsymbol{c}_k \sim \mathcal{N}(\boldsymbol{0}_m, \boldsymbol{I}_m)$ and then normalized as $\boldsymbol{c}_k / \|\boldsymbol{c}_k\|$.

(Orthogonal) Random subspace precoding (`RSP`) consists in considering the singular value decomposition of the matrix $\boldsymbol{\Psi} \triangleq \boldsymbol{\Sigma}_k^{-1} \boldsymbol{J}_k(\boldsymbol{\theta}_0)$, namely $\boldsymbol{\Psi} = \boldsymbol{U}_\Psi \boldsymbol{\Lambda}_\Psi \boldsymbol{V}_\Psi^T$, and randomly sampling $m_k \le p$ columns from $\boldsymbol{U}_\Psi$. By doing so, the orthogonal compression matrix will be guaranteed to generate *part of the subspace* where the $\boldsymbol{\gamma}_k$ *always* lies. In view of the aforementioned assumptions, the above method can be used only for $m_k \le p$.

(Orthogonal) Top(-directions) subspace precoding (`TSP`) similarly considers the singular value decomposition of the matrix $\boldsymbol{\Psi}$, namely $\boldsymbol{\Psi} = \boldsymbol{U}_\Psi \boldsymbol{\Lambda}_\Psi \boldsymbol{V}_\Psi^T$, but rather uses the columns of $\boldsymbol{U}_\Psi$ associated to the m_k *highest singular values*. In this way, the orthogonal compression matrix will be guaranteed to generate *part of the subspace* where the vector $\boldsymbol{\gamma}_k$ *always* lies, while picking the m_k directions corresponding the highest sensitivity with respect to deviations of $(\boldsymbol{\theta}_1 - \boldsymbol{\theta}_0)$. Similarly as `TSP`, the above method can be used only for $m_k \le p$.

Remarks: we stress that we do not consider sign-assisted precoding [33] and `UNF` precoding in the multi-bit case. Indeed, the former retains the same implementation problems as in the one-bit case, while for the latter there is no trival extension of uniform-direction concept.

VI. SIMULATION RESULTS

A. Setup and Upper-Bounds Definition

In this section, we numerically investigate the proposed fusion schemes for the VL model described in Eq. (3), with parameters

$m = 8$ (size of the observation vector) and $p = 3$ (size of the unknown vector signal). To this end, we consider a WSN scenario with $K = 15$ sensors.

To reproduce a *heterogeneous* scenario, the noise covariance $\boldsymbol{\Sigma}_k$ of each sensor is randomly generated following an exponentially-correlated Gaussian model, namely $\boldsymbol{\Sigma}_k = (\sigma_c^2 \boldsymbol{M}_{c,k} + \sigma_n^2 \boldsymbol{I}_N)$, where $\sigma_c^2 = (9/10)$ is the clutter power and $\sigma_n^2 = (1/10)$ is the thermal noise power. Additionally, the (r,s)th element of $\boldsymbol{M}_{c,k}$ is given by $(\varrho_k)^{|r-s|}$, where $\varrho_k \sim \mathcal{U}(0.7, 0.9)$. Initially, we assume ideal BEP channels ($P_{e,k} = 0, k \in \mathcal{K}$) between sensors and the FC.

In the simulated scenarios, when the hypothesis $\mathcal{H}_1$ holds, the vector parameter is sampled as $\boldsymbol{\theta} \sim \mathcal{N}(\boldsymbol{0}_3, \boldsymbol{I}_3)$ at each run and scaled such to ensure the desired *sensing SNR* (assumed to be the same for all the sensors). The latter is defined as $\mathrm{SNR} \triangleq \frac{\|\boldsymbol{\theta}\|^2}{\mathrm{tr}(\boldsymbol{\Sigma}_k)/m}$. The results are based on 10^5 Monte Carlo runs.

For the sake of completeness, to assess the quantization and reporting effects, we consider the following *upper bound*. Specifically, we consider a GLRT/Rao test having all the measurements $\boldsymbol{x}_1, \dots, \boldsymbol{x}_K$ ideally available at the FC.[3] Its explicit expression for the VL model is (we do not report the proof for sake of brevity, since it can be found in [23]):

$$\Lambda^{\mathrm{ub,vl}} =$$

$$\left(\sum_{k=1}^{K} \boldsymbol{x}_k^T \boldsymbol{\Sigma}_k^{-1} \boldsymbol{H}_k \right) \left(\sum_{k=1}^{K} \boldsymbol{H}_k^T \boldsymbol{\Sigma}_k^{-1} \boldsymbol{H}_k \right)^{-1} \left(\sum_{k=1}^{K} \boldsymbol{H}_k^T \boldsymbol{\Sigma}_k^{-1} \boldsymbol{x}_k \right) \tag{57}$$

We remark that in the general measurement case described by Eq. (1), two different upper bounds (either based on GLRT or Rao test) should be considered.[4]

B. Results and Discussion

The present subsection investigates the performance of GLR and Rao tests by analyzing their trends with relevant WSN parameters, including (i) the different compression heuristics, (ii) the sensing SNR, (iii) the quantization resolution m_k and (iv) the degree of channel impairments.

Receiver Operating Characteristic (ROC) analysis: Initially, in Fig. 2, we compare the ROCs of GLR and Rao tests for the specified VL model, focusing on the single-bit case ($m_k = 1$) and a moderate sensing $\mathrm{SNR} = 5$dB. Regarding the optimization of hyperplane-based quantizers, we consider $\tau_k = 0$ and investigate the four heuristic approaches for the design of the compression vectors $\boldsymbol{c}_k$'s. First, results highlight no significant performance difference between GLR and Rao tests over all the (P_{F_0}, P_{D_0}) plane. This observation applies to all the compression vector choices considered. Additionally, it

---

[3]Indeed, in this special case, Rao test and GLRT are statistically equivalent [23]

[4]Specifically, GLR expression is $\Lambda_G^{\mathrm{ub}} \triangleq \sum_{k=1}^{K} \{2 \boldsymbol{x}_k^T \boldsymbol{\Sigma}_k^{-1} \boldsymbol{g}_k(\hat{\boldsymbol{\theta}}) - \boldsymbol{g}_k(\hat{\boldsymbol{\theta}})^T \boldsymbol{\Sigma}_k^{-1} \boldsymbol{g}_k(\hat{\boldsymbol{\theta}})\}$ where $\hat{\boldsymbol{\theta}}$ denotes the usual ML estimate. Differently, Rao statistic is given as $\Lambda_R^{\mathrm{ub}} \triangleq \boldsymbol{v}(\boldsymbol{x}; \boldsymbol{\theta}_0)^T \{\sum_{k=1}^{K} \boldsymbol{J}_k(\boldsymbol{\theta}_0)^T \boldsymbol{\Sigma}_k^{-1} \boldsymbol{J}_k(\boldsymbol{\theta}_0)\} \boldsymbol{v}(\boldsymbol{x}; \boldsymbol{\theta}_0)$ where $\boldsymbol{v}(\boldsymbol{x}; \boldsymbol{\theta}_0) \triangleq \sum_{k=1}^{K} \boldsymbol{J}_k(\boldsymbol{\theta}_0)^T \boldsymbol{\Sigma}_k^{-1} (\boldsymbol{x}_k - \boldsymbol{g}_k(\boldsymbol{\theta}_0))$.
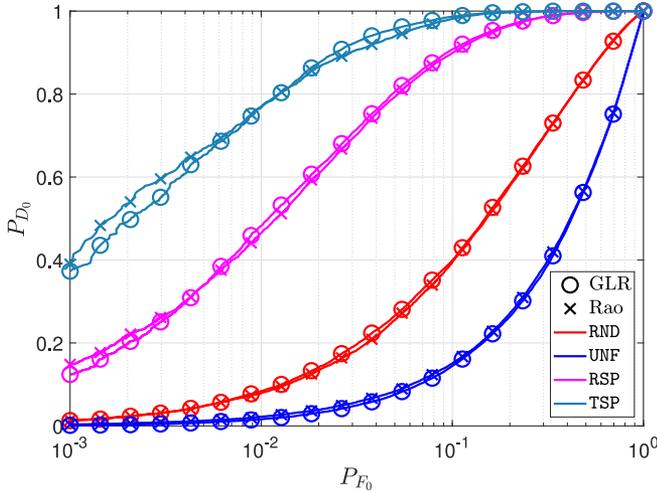
Fig. 2. P_{D_0} vs. P_{F_0} for GLR (∘ markers) and Rao (× markers) tests. Random (RND), uniform (UNF), random subspace (RSP) and top subspace (TSP) precoding approaches are compared. WSN with $K = 15$ sensors, $m = 8$ and $p = 3$, and the sensing SNR = 5 dB. One bit-quantization ($m_k = 1$) and ideal BSCs are considered ($P_{e,k} = 0$).
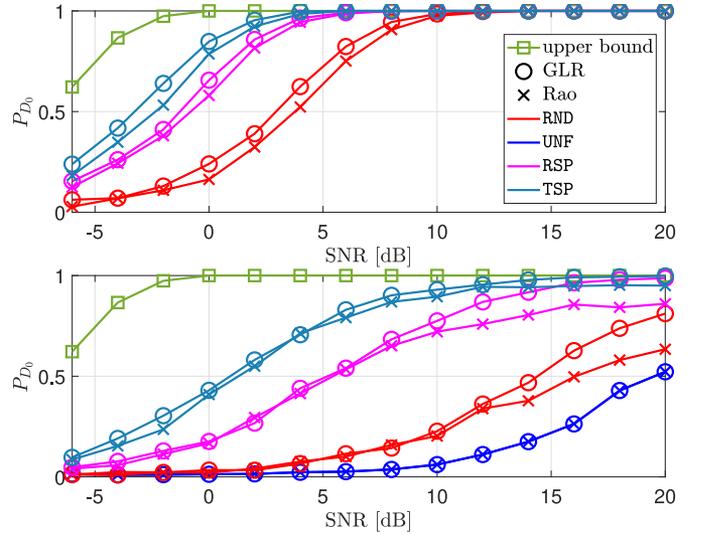

Fig. 3. P_{D_0} vs. SNR [dB] for GLR (∘ markers) and Rao (× markers) tests, subject to $P_{F_0} = 0.01$. Top and bottom plots refer to two-bit ($m_k = 2$) and one-bit quantization ($m_k = 1$), respectively. Random (RND), Uniform (UNF), Random Subspace (RSP) and Top Subspace (TSP) precoding approaches are compared. WSN with $K = 15$ sensors, $m = 8$ and $p = 3$. Ideal BSCs are considered ($P_{e,k} = 0$).

is apparent the better performance of both RSP and TSP, due to their specialization on the subspace where the vector signal $\boldsymbol{\theta}$ lies. In particular, the latter outperforms the former due to the alignment with the highest principal direction of the sensing subspace $\boldsymbol{\Sigma}_k^{-1} \boldsymbol{H}_k$.

Detection rate vs. sensing SNR: We then compare the performance of GLR and Rao tests by considering the detection rate P_{D_0} and its improvement with the sensing SNR, focusing on the four compression heuristics adopted. Herein, the false-alarm rate is set[5] to $P_{F_0} = 0.01$. The corresponding results are shown in Fig. 3. Additionally, we assess the possible benefits of multi-bit quantization, namely when moving from $m_k = 1$ (bottom plot) to $m_k = 2$ (top plot). Also in this case the quantizer thresholds are optimally (from an asymptotic viewpoint) chosen as $\tau_k^\star = 0$. For the sake of complete comparison, also the P_{D_0} performance of the upper bound described in Eq. (57) is reported. Results show that (i) all compression methods and (ii) both rules benefit from (sensing) SNR increase, with GLR performing slightly better. However, the Rao test is far more efficient than the GLRT from the viewpoint of computation burden and complexity. The relative trend among the four compression methods is retained for the whole SNR range considered. When moving from $m_k = 1$ to $m_k = 2$, there is a relative shift of all methods toward the performance of the upper bound. Still, the latter performance cannot be approached due to the fact that the upper bound has available m-dimensional and full-precision (viz. unquantized) information for performing the fusion process.
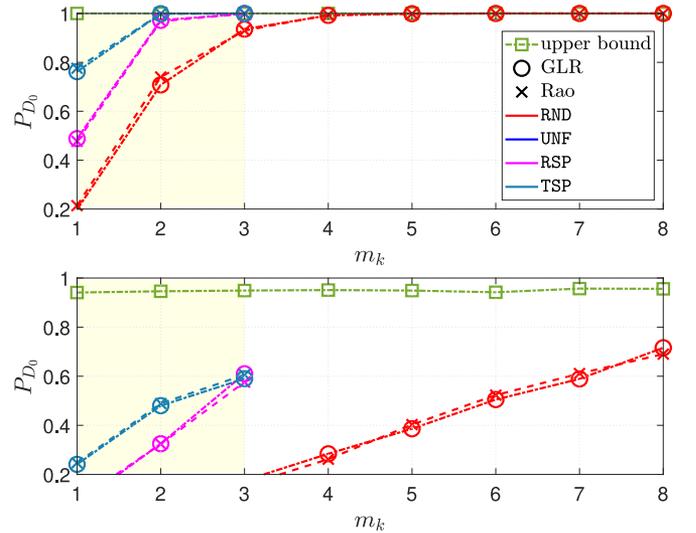

Fig. 4. P_{D_0} vs. m_k for GLR (∘ markers) and Rao (× markers) tests, subject to $P_{F_0} = 0.01$. Top and bottom plots refer to SNR = 5 dB (moderate SNR) and SNR = −3 dB (low SNR), respectively. Random (RND), uniform (UNF), random subspace (RSP) and top subspace (TSP) precoding approaches are compared. Shaded area indicates number of quantization bits ≤ of the signal subspace size. WSN with $K = 15$ sensors, $m = 8$ and $p = 3$. Ideal BSCs are considered ($P_{e,k} = 0$).

Detection rate vs. quantization resolution: Subsequently, we focus on the effect of increasing quantization resolution on detection performance in Fig. 4. To this end, we report P_{D_0} vs. m_k for both the fusion rules, setting the false-alarm rate to $P_{F_0} = 0.01$. The effect of RND, RSP and TSP compressions strategies is investigated herein (recall that UNF is only defined for $m_k = 1$). To appreciate such effect in different conditions,

---

[5] When a given false-alarm rate α_{FA} needs to be ensured, we generate $N_{F_0} = 10^2 / \alpha_{\mathrm{FA}}$ runs according to the hypothesis $\mathcal{H}_0$. For each run, the corresponding statistic Λ is calculated. Then, all the samples of the decision statistic are sorted increasingly to obtain an empirical CDF of the random variable $\Lambda | \mathcal{H}_0$, defined as $\Pr(\Lambda < \gamma \,|\, \mathcal{H}_0)$. Accordingly, the desired γ is chosen as $\gamma : \Pr(\Lambda < \gamma \,|\, \mathcal{H}_0) = (1 - \alpha_{\mathrm{FA}})$. This corresponds to choosing γ from the empirical CDF as the value corresponding to the index closest to $N_{F_0}(1 - \alpha_{\mathrm{FA}})$.
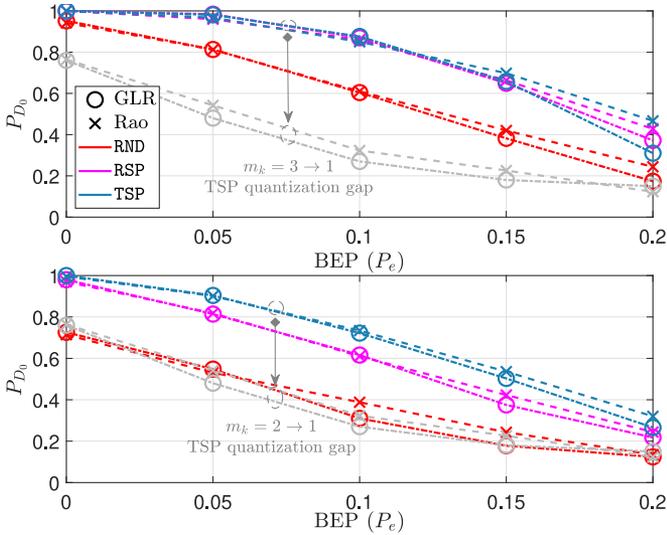
Fig. 5. P_{D_0} vs. P_e for GLR (∘ markers) and Rao (× markers) tests, subject to $P_{F_0} = 0.01$. Top and bottom plots refer to three-bit ($m_k = 3$) and two-bit quantization ($m_k = 2$), respectively. Random (RND), random subspace (RSP) and top subspace (TSP) precoding approaches are compared. To assess the gain due to finer quantization, in light grey we also report the corresponding GLR and Rao performance when only one-bit quantization (with TSP precoding) is used. A WSN with $K = 15$ sensors, $m = 8$ and $p = 3$, and sensing SNR $= 5$ dB is considered.

we report performance corresponding to *moderate* and *low* SNR values, corresponding to SNR $= 5$ dB and SNR $= -3$ dB, reported in top and bottom plots, respectively. Results in both plots highlight the clear benefit of using both Rao and GLR tests which leverage multi-bit quantization. Specifically, in the moderate SNR case, three bits are sufficient for RSP and TSP to achieve ideal performance, whereas more bits are needed by RND to achieve the same (ideal) detection rate. Differently, in the low SNR case, although beneficial, the performance gain with m_k is not able to reach ideal (and also the upper bound) performance. We recall that RND compression is also defined for $p < m_k < m$, as opposed to RSP and TSP.

Detection rate vs. BEP: Finally, we assess the performance of both GLR and Rao fusion rules with respect to communication channel impairments (i.e. $P_{e,k} \neq 0$). To this end, in Fig. 5 we show P_{D_0} vs. P_e (we assume the same BEP for all the sensors, namely $P_{e,k} = P_e$, $\forall k \in \mathcal{K}$) for both the fusion rules and the four compression methods investigated. For the sake of completeness, we consider $m_k = 2$ (bottom) and $m_k = 3$ (top) quantization bit cases, so as to appreciate the effects of channel errors on different resolutions. As in the previous analyses, we consider a false-alarm rate equal to $P_{F_0} = 0.01$. Results highlight that channel-errors may degrade system detection performance (independently on the rule implemented at the FC), e.g. considering $m_k = 3$ and RSP/TSP precoders there is detection loss of $\approx 20\%$ when there is $P_e = 0.1$. However, the gains due to multi-bit quantization are still apparent even when $P_e \neq 0$. For instance, when $P_e = 0.1$ and TSP precoding is adopted, the detection rate with three-bit (resp. two-bit) quantization improves over one-bit counterparts by $\approx 60\%$ (resp. $\approx 40\%$).

VII. CONCLUSIONS AND FURTHER DIRECTIONS

In this paper, we considered decentralized detection of an unknown vector $\boldsymbol{\theta}$ by sensor fusion of data from nodes associated to a non-linear vector measurement model. These sensors were assumed to employ hyperplane-based quantizers and to be affected by impaired communication channels. The Rao fusion rule was derived and proposed herein as a *simpler* (and thus attractive) *alternative* to GLRT, since it is in closed form (even under such general model) and obviates the need for cumbersome ML estimation.

Additionally, we provided the explicit expression of the asymptotic (weak-signal) performance of Rao (viz. GLRT) fusion rule, here exploited to optimize the system detection performance (namely, the non-centrality parameter) by tuning the parameters (τ_k, $\boldsymbol{c}_k$) of each sensor quantizer. It was shown that, while an optimized expression for kth threshold can be obtained explicitly as $\tau_k^\star = \boldsymbol{c}_k^T \boldsymbol{g}_k(\boldsymbol{\theta}_0)$, the optimal $\boldsymbol{c}_k^\star$ depends in turn on the unknown vector signal $\boldsymbol{\theta}$. Hence, we resorted to four reasonable heuristics for its design (i.e. RND, UNF, RSP and TSP). It was shown through simulations that the Rao test, in addition to being asymptotically equivalent to the GLRT, achieves similar performance trends in the case of a finite number of sensors (but with considerable less computational burden). Additionally, we observed that RSP and TSP precoders outperform RND (and UNF in the single bit case), due to the knowledge of the subspace where the (unknown) vector signal lies.

Furthermore, our study also demonstrated the advantage of multi-bit quantization against one-bit quantization, as well as its *practical feasibility*, by deriving a Rao test for this generalized setup. According to the results, even a few (two or three) quantization bits are sufficient to provide relevant performance gains in a WSN with perfect reporting channels. Differently, the presence of errors on the reporting phase increases the performance gap with the upper bound (i.e. the fully-precision, unquantized benchmark).

Future directions will include design of Rao test for alternative, (even) more general and realistic measurement & channel models: (a) sensing models enjoying sparsity [21]; (b) energy-efficient censoring sensors [41]; (c) time-correlated reporting channels [42]; (d) design of online precoders $\boldsymbol{c}_k$'s [40]; (e) unknown random signal parameters [43]; (f) incompletely-specified noise PDFs.

APPENDIX
PROOF OF PROPOSITION 1 (SCORE VECTOR)

Capitalizing the independence among nodes' data, we obtain the following simplified form of the score function:

$$\boldsymbol{\delta}(\boldsymbol{y}; \boldsymbol{\theta}) = \sum_{k=1}^{K} \frac{\partial \ln P(y_k; \boldsymbol{\theta})}{\partial \boldsymbol{\theta}} \qquad (58)$$

Then, by defining $a_k \triangleq \boldsymbol{c}_k^T \boldsymbol{g}_k(\boldsymbol{\theta})$, kth sensor contribution to score vector can be expressed as:

$$\frac{\partial \ln P(y_k; \boldsymbol{\theta})}{\partial \boldsymbol{\theta}} = \frac{\partial \ln P(y_k; \boldsymbol{\theta})}{\partial a_k} \frac{\partial a_k}{\partial \boldsymbol{\theta}} \qquad (59)$$

Furthermore, exploiting Eqs. (7) and (8), it provides:

$$\frac{\partial \ln P\left(y_k;\boldsymbol{\theta}\right)}{\partial a_k} = \frac{\left(y_k - \psi_k\left(\boldsymbol{\theta}\right)\right)\zeta_k\, p_{v_k}\left(\tau_k - \boldsymbol{c}_k^T \boldsymbol{g}_k\left(\boldsymbol{\theta}\right)\right)}{\psi_k\left(\boldsymbol{\theta}\right)\left(1 - \psi_k\left(\boldsymbol{\theta}\right)\right)} \tag{60}$$

where we have defined $\zeta_k \triangleq \left(1 - 2\epsilon_k\right)$.

Finally, by noting that $\frac{\partial a_k}{\partial \boldsymbol{\theta}} = \boldsymbol{J}_k^T(\boldsymbol{\theta})\boldsymbol{c}_k$ and exploiting Eq. (60), provides the desired result in Eq. (11).

APPENDIX B
PROOF OF PROPOSITION 2 (FIM)

We start from FIM general definition [44]:

$$\boldsymbol{I}\left(\boldsymbol{\theta}\right) \triangleq \mathbb{E}\left\{\boldsymbol{\delta}(\boldsymbol{y};\boldsymbol{\theta})\,\boldsymbol{\delta}(\boldsymbol{y};\boldsymbol{\theta})^T\right\} \tag{61}$$

Then, exploiting independence among the received bits, we obtain the simplified (additive) form:

$$\boldsymbol{I}\left(\boldsymbol{\theta}\right) = \sum_{k=1}^{K}\mathbb{E}\left\{\frac{\partial \ln P\left(y_k;\boldsymbol{\theta}\right)}{\partial\boldsymbol{\theta}}\left(\frac{\partial \ln P\left(y_k;\boldsymbol{\theta}\right)}{\partial\boldsymbol{\theta}}\right)^T\right\}, \tag{62}$$

Each of the K terms in the above equation can be obtained by resorting to Eq. (60), which thus gives the intermediate expression:

$$\boldsymbol{I}\left(\boldsymbol{\theta}\right) = \sum_{k=1}^{K}\left\{\mathbb{E}_{y_k}\left\{\frac{\left(\psi_k\left(\boldsymbol{\theta}\right) - y_k\right)^2}{\psi_k^2\left(\boldsymbol{\theta}\right)\left(1 - \psi_k\left(\boldsymbol{\theta}\right)\right)^2}\right\}\right.$$
$$\left.\zeta_k^2\, p_{v_k}^2\left(\tau_k - \boldsymbol{c}_k^T \boldsymbol{g}_k\left(\boldsymbol{\theta}\right)\right)\boldsymbol{J}_k^T\left(\boldsymbol{\theta}\right)\boldsymbol{c}_k\boldsymbol{c}_k^T\boldsymbol{J}_k\left(\boldsymbol{\theta}\right)\right\}. \tag{63}$$

On the other hand, the expectation in Eq. (63) is simply computed as:

$$\mathbb{E}_{y_k}\left\{\frac{\left(\psi_k\left(\boldsymbol{\theta}\right) - y_k\right)^2}{\psi_k^2\left(\boldsymbol{\theta}\right)\left(1 - \psi_k\left(\boldsymbol{\theta}\right)\right)^2}\right\} = \frac{1}{\psi_k\left(\boldsymbol{\theta}\right)\left(1 - \psi_k\left(\boldsymbol{\theta}\right)\right)} \tag{64}$$

Replacing the above result in Eq. (63) gives the final result in (14). This concludes the proof.

REFERENCES

[1] P. K. Varshney, *Distributed Detection and Data Fusion*. New York, NY, USA: Springer-Verlag, 1996.

[2] S. H. Javadi, "Detection over sensor networks: a tutorial," *IEEE Aerosp. Elect. Syst. Mag.*, vol. 31, no. 3, pp. 2–18, Mar. 2016.

[3] D. Ciuonzo and P. Salvo Rossi, Eds., *Data Fusion in Wireless Sensor Networks: A Statistical Signal Processing Perspective* (series on Control, Robotics & Sensors). London, U.K.: Institution of Engineering and Technology (IET), 2019.

[4] R. Viswanathan and P. K. Varshney, "Distributed detection with multiple sensors: Part I-fundamentals," *Proc. IEEE*, vol. 85, no. 1, pp. 54–63, 1997.

[5] D. Ciuonzo, G. Papa, G. Romano, P. Salvo Rossi, and P. Willett, "One-bit decentralized detection with a Rao test for multisensor fusion," *IEEE Signal Process. Lett.*, vol. 20, no. 9, pp. 861–864, Sep. 2013.

[6] J. Fang, Y. Liu, H. Li, and S. Li, "One-bit quantizer design for multisensor GLRT fusion," *IEEE Signal Process. Lett.*, vol. 20, no. 3, p. 257260, Mar. 2013.

[7] G. Ferrari, M. Martalo, and R. Pagliari, "Decentralized detection in clustered sensor networks," *IEEE Trans. Aerosp. Electron. Syst.*, vol. 47, no. 2, pp. 959–973, Apr. 2011.

[8] S. A. Aldalahmeh, S. O. Al-Jazzar, D. McLernon, S. A. R. Zaidi, and M. Ghogho, "Fusion rules for distributed detection in clustered wireless sensor networks with imperfect channels," *IEEE Trans. Signal Inf. Process. Netw.*, vol. 5, no. 3, pp. 585–597, Sep. 2019.

[9] R. Niu and P. K. Varshney, "Distributed detection and fusion in a large wireless sensor network of random size," *EURASIP J. Wireless Commun. Netw.*, vol. 2005, no. 4, pp. 462–472, 2005.

[10] R. Niu and P. K. Varshney, "Performance analysis of distributed detection in a random sensor field," *IEEE Trans. Signal Process.*, vol. 56, no. 1, pp. 339–349, Jan. 2008.

[11] A. Goel, A. Patel, K. G. Nagananda, and P. K. Varshney, "Robustness of the counting rule for distributed detection in wireless sensor networks," *IEEE Signal Process. Lett.*, vol. 25, no. 8, pp. 1191–1195, Aug. 2018.

[12] D. Ciuonzo, A. De Maio, and P. Salvo Rossi, "A systematic framework for composite hypothesis testing of independent Bernoulli trials," *IEEE Signal Process. Lett.*, vol. 22, no. 9, pp. 1249–1253, Sep. 2015.

[13] B. Chen, R. Jiang, T. Kasetasem, and P. K. Varshney, "Channel aware decision fusion in wireless sensor networks," *IEEE Trans. Signal Process.*, vol. 52, no. 12, pp. 3454–3458, Dec. 2004.

[14] D. Ciuonzo, G. Romano, and P. Salvo Rossi, "Channel-aware decision fusion in distributed MIMO wireless sensor networks: Decode-and-fuse vs. decode-then-fuse," *IEEE Trans. Wireless Commun.*, vol. 11, no. 8, pp. 2976–2985, Aug. 2012.

[15] D. Ciuonzo, G. Romano, and P. Salvo Rossi, "Optimality of received energy in decision fusion over Rayleigh fading diversity MAC with non-identical sensors," *IEEE Trans. Signal Process.*, vol. 61, no. 1, pp. 22–27, Jan. 2013.

[16] R. Niu, P. K. Varshney, and Q. Cheng, "Distributed detection in a large wireless sensor network," *Inf. Fusion*, vol. 7, no. 4, pp. 380–394, 2006.

[17] L. Hu, X. Wang, and S. Wang, "Decentralized underwater target detection and localization," *IEEE Sens. J.*, 2020.

[18] S. G. Iyengar, R. Niu, and P. K. Varshney, "Fusing dependent decisions for hypothesis testing with heterogeneous sensors," *IEEE Trans. Signal Process.*, vol. 60, no. 9, pp. 4888–4897, Sep. 2012.

[19] F. Gao, L. Guo, H. Li, J. Liu, and J. Fang, "Quantizer design for distributed GLRT detection of weak signal in wireless sensor networks," *IEEE Trans. Wireless. Commun.*, vol. 14, no. 4, pp. 2032–2042, Apr. 2015.

[20] G. Wang, J. Zhu, R. S. Blum, P. Willett, S. Marano, V. Matta, and P. Braca, "Signal amplitude estimation and detection from unlabeled binary quantized samples," *IEEE Trans. Signal Process.*, vol. 66, no. 16, pp. 4291–4303, Aug. 2018.

[21] H. Zayyani, F. Haddadi, and M. M. Korki, "Double detector for sparse signal detection from one-bit compressed sensing measurements," *IEEE Signal Process. Lett.*, vol. 23, no. 11, pp. 1637–1641, Nov. 2016.

[22] S. Li, X. Li, X. Wang, and J. Liu, "Decentralized sequential composite hypothesis test based on one-bit communication," *IEEE Trans. Inf. Theory*, vol. 63, no. 6, pp. 3405–3424, Jun. 2017.

[23] S. M. Kay, *Fundamentals of Statistical Signal Processing, Volume 2: Detection Theory*. Upper Saddle River, NJ, USA: Prentice Hall PTR, Jan. 1998.

[24] X. Cheng, D. Ciuonzo, and P. Salvo Rossi, "Multi-bit decentralized detection through fusing smart & dumb sensors based on Rao test," *IEEE Trans. Aerosp. Electron. Syst.*, vol. 56, no. 2, pp. 1391–1405, Apr. 2020.

[25] D. Ciuonzo, P. Salvo Rossi, and P. Willett, "Generalized Rao test for decentralized detection of an uncooperative target," *IEEE Signal Process. Lett.*, vol. 24, no. 5, pp. 678–682, May 2017.

[26] X. Cheng, D. Ciuonzo, P. Salvo Rossi, X. Wang, and L. Shi, "Multi-bit decentralized detection of a non-cooperative moving target through a generalized Rao test," in *Proc. IEEE 11th Sensor Array Multichannel Signal Process. (SAM)*, 2020, pp. 1–5.

[27] L. Hu, J. Zhang, X. Wang, S. Wang, and E. Zhang, "Decentralized truncated one-sided sequential detection of a noncooperative moving target," *IEEE Signal Process. Lett.*, vol. 25, no. 10, pp. 1490–1494, Oct. 2018.

[28] S. Laitrakun, "Rao-Test fusion rules of uncensored decisions transmitted over a collision channel," in *Proc. 21st IEEE Int. Symp. Wireless Pers. Multimedia Commun.*, 2018, pp. 495–500.

[29] X. Wang, G. Li, and P. K. Varshney, "Detection of sparse stochastic signals with quantized measurements in sensor networks," *IEEE Trans. Signal Process.*, vol. 67, no. 8, pp. 2210–2220, Apr. 2019.

[30] X. Wang, G. Li, C. Quan, and P. K. Varshney, "Distributed detection of sparse stochastic signals with quantized measurements: The generalized gaussian case," *IEEE Trans. Signal Process.*, vol. 67, no. 18, pp. 4886–4898, Sep. 2019.

[31] S. Laitrakun, "Decision fusion for composite hypothesis testing in wireless sensor networks over a shared and noisy collision channel," *Int. J. Distrib. Sensor Netw.*, vol. 16, no. 7, pp. 1–16, 2020.

[32] J. Fang and H. Li, "Hyperplane-based vector quantization for distributed estimation in wireless sensor networks," *IEEE Tran. Inf. Theory*, vol. 55, no. 12, pp. 5682–5699, Dec. 2009.

[33] J. Fang, X. Li, H. Li, and L. Huang, "Precoding for decentralized detection of unknown deterministic signals," *IEEE Trans. Aerosp. Elect. Syst.*, vol. 50, no. 3, pp. 2116–2128, Jul. 2014.

[34] A. Ribeiro and G. B. Giannakis, "Bandwidth-constrained distributed estimation for wireless sensor networks-part I: Gaussian case," *IEEE Trans. Signal Process.*, vol. 54, no. 3, pp. 1131–1143, Mar. 2006.

[35] A. Ribeiro and G. B. Giannakis, "Bandwidth-constrained distributed estimation for wireless sensor networks-part II: Unknown probability density function," *IEEE Trans. Signal Process.*, vol. 54, no. 7, p. 27842796, Jul. 2006.

[36] H. Chen and P. K. Varshney, "Performance limit for distributed estimation systems with identical one-bit quantizers," *IEEE Trans. Signal Process.*, vol. 58, no. 1, p. 466471, Jan. 2010.

[37] S. Kar, H. Chen, and P. K. Varshney, "Optimal identical binary quantizer design for distributed estimation," *IEEE Trans. Signal Process.*, vol. 60, no. 7, pp. 3896–3901, Jul. 2012.

[38] D. Ciuonzo, G. Romano, and P. Salvo Rossi, "Performance analysis and design of maximum ratio combining in channel-aware MIMO decision fusion," *IEEE Trans. Wireless Commun.*, vol. 12, no. 9, pp. 4716–4728, Sep. 2013.

[39] H. C. Papadopoulos, G. W. Wornell, and A. V. Oppenheim, "Sequential signal encoding from noisy measurements using quantizers with dynamic bias control," *IEEE Trans. Inf. Theory*, vol. 47, no. 3, pp. 978–1002, Mar. 2001.

[40] P. Khanduri, L. N. Theagarajan, and P. K. Varshney, "Online design of optimal precoders for high dimensional signal detection," *IEEE Trans. Signal Process.*, vol. 67, no. 15, pp. 4122–4135, Aug. 2019.

[41] C. Rago, P. Willett, and Y. Y. Bar-Shalom, "Censoring sensors: A low-communication-rate scheme for distributed detection," *IEEE Trans. Aerosp. Elect. Syst.*, vol. 32, no. 2, pp. 554–568, Apr. 1996.

[42] N. Biswas, P. Ray, and P. K. Varshney, "Distributed detection over channels with memory," *IEEE Signal Process. Lett.*, vol. 22, no. 12, pp. 2494–2498, Dec. 2015.

[43] F. Gao, L. Guo, H. Li, and J. Fang, "One-bit quantization and distributed detection with an unknown scale parameter," *MDPI Algorithms*, vol. 8, no. 3, pp. 621–631, 2015.

[44] S. M. Kay, *Fundamentals of Statistical Signal Processing, Volume 1: Estimation Theory*. Upper Saddle River, New Jersey: Prentice Hall PTR, 1993.

Abdolreza Mohammadi (Member, IEE) received the B.Sc. degree in electrical engineering from Ferdowsi University and the M.Sc. and Ph.D. degrees in communication systems engineering from Yazd University, Yazd, Iran. From December 2011 to June 2012, he was a Visiting Ph.D. Student with the School of Electrical and Electronic Engineering, Nanyang Technological University, Singapore. He is currently working as an Assistant Professor in electrical engineering with the University of Bojnord, Bojnord, Iran. His research interests include fuzzy probability, statistical signal processing, information fusion, and wireless sensor network.

Pierluigi Salvo Rossi (Senior Member, IEEE) was born in Naples, Italy, in 1977. He received the Dr.Eng. degree (*summa cum laude*) in telecommunications engineering and the Ph.D. degree in computer engineering from the University of Naples "Federico II," Italy, in 2002 and 2005, respectively. He held visiting appointments with the Department of Electrical and Computer Engineering, Drexel University, USA; at the Department of Electrical and Information Technology, Lund University, Sweden; at the Department of Electronics and Telecommunications, Norwegian University of Science and Technology (NTNU), Norway; and at the Excellence Center for Wireless Sensor Networks, Uppsala University, Sweden. From 2005 to 2008, he held Postdoctoral positions with the Department of Computer Science and Systems, University of Naples "Federico II," Italy; with the Department of Information Engineering, Second University of Naples, Italy; and with the Department of Electronics and Telecommunications, NTNU, Norway. From 2008 to 2014, he was an Assistant Professor (tenured in 2011) in telecommunications with the Department of Industrial and Information Engineering, Second University of Naples, Italy. From 2014 to 2016, he was an Associate Professor in signal processing with the Department of Electronics and Telecommunications, NTNU, Norway. From 2016 to 2017, he was a Full Professor in signal processing with the Department Electronic Systems, NTNU, Norway. From 2017 to 2019, he was a Principal Engineer with the Department of Advanced Analytics and Machine Learning, Kongsberg Digital AS, Norway. Since 2019, he has been a Full Professor of statistical machine learning with the Department of Electronic Systems, NTNU, Norway, and also the Director of IoT@NTNU. His research interests fall within the areas of communication theory, data fusion, machine learning, and signal processing. Dr. Rossi serves as an Executive Editor for the IEEE COMMUNICATIONS LETTERS since 2019, an Area Editor for the IEEE OPEN JOURNAL OF THE COMMUNICATIONS SOCIETY since 2019, an Associate Editor for the IEEE TRANSACTIONS ON SIGNAL AND INFORMATION PROCESSING OVER NETWORKS since 2019, and an Associate Editor for the IEEE TRANSACTIONS ON WIRELESS COMMUNICATIONS since 2015. He was a Senior Editor from 2016 to 2019 and an Associate Editor from 2012 to 2016 of the IEEE COMMUNICATIONS LETTERS. He was awarded as an Exemplary Senior Editor of the IEEE COMMUNICATIONS LETTERS in 2018.

Domenico Ciuonzo (Senior Member, IEEE) received the Ph.D. degree in electronic engineering from the University of Campania "L. Vanvitelli," Italy. He is currently an Assistant professor with University of Napoli Federico II. Since 2011, he has been holding several Visiting Researcher appointments. Since 2014, he has been (Area) Editor of several IEEE, IET, and ELSEVIER journals. His research interests include data fusion, statistical signal processing, wireless sensor networks, Internet of Things and machine learning. Dr. Ciuonzo was the recipient of Best Paper Awards from IEEE ICCCS (2019) and Elsevier Computer Networks (2020), Exceptional Service Award from IEEE Aerospace and Electronic Systems Society (2019), and Early-Career Technical Achievement award from IEEE Sensors Council for Sensor Networks/systems (2020).

S. Hamed Javadi (Member, IEEE) received the B.S. degree in electrical engineering from the Ferdowsi University of Mashhad, Iran, in 2005, the M.S. degree from Electronic Department, K.N. Toosi University of Technology, Iran, in 2008 and the Ph.D. degree from the Ferdowsi University of Mashhad, Iran, in 2013. He was an Assistant Professor with the University of Bojnord since 2013 to 2019, where He was involved in several international projects. Hamed is currently working as a Postdoctoral Researcher with the Environment Department, Ghent University. His fields of expertise include statistical signal processing, data fusion, and machine learning.